University College Dublin, 11 May 2016

Freak waves in negative-ion plasmas: an experiment revisited

Ioannis Kourakis

Queen's University Belfast, Centre for Plasma Physics, Northern Ireland, UK

in collaboration with

Ibrahem El-Kamash, Michael McKerr and Brian Reville

Queen's University Belfast

Outline

1. **Introduction**
   * *Rogue waves* (or *freak waves)* – physical setting & preliminaries
   * *Nonlinear amplitude modulation*: basic phenomenology
   * Framework for *electrostatic wavepacket modulation*
2. **Negative-ion plasmas & modulation:** modelling and discrepancies
3. **Analytical framework & modeling** – from first principles
4. **Analytical models for rogue waves**
5. **Discussion & Summary**

Intro #1: Rogue waves – an emerging unifying concept

- *Rogue waves* are localized excitations (events) of extreme amplitude, exceeding twice the average strength of background turbulence level;

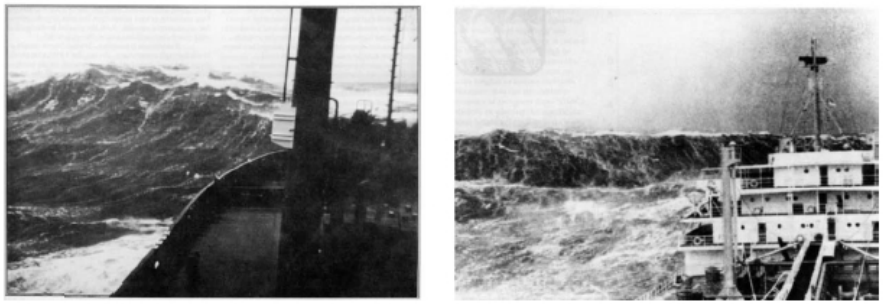

Fig. 2. Various photos of rogue waves.

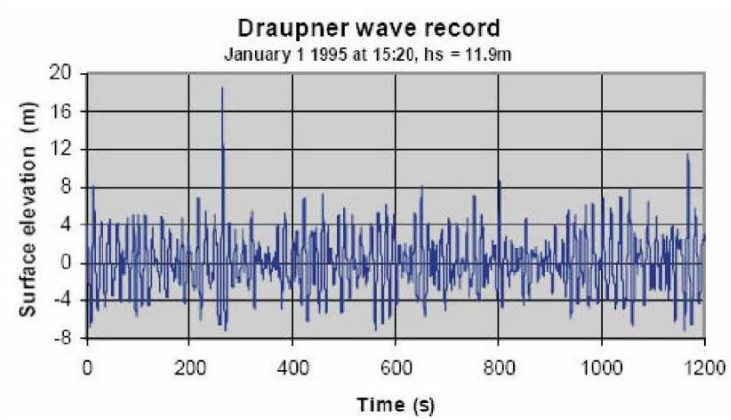

Data from the Draupner platform event in Norway (Jan. 1995).

Credit: Kharif & Pelinovsky, Eur. Journal of Mechanics B/Fluids **22**, 603 (2003).

Catastrophic ship encounters with rogue waves - stats

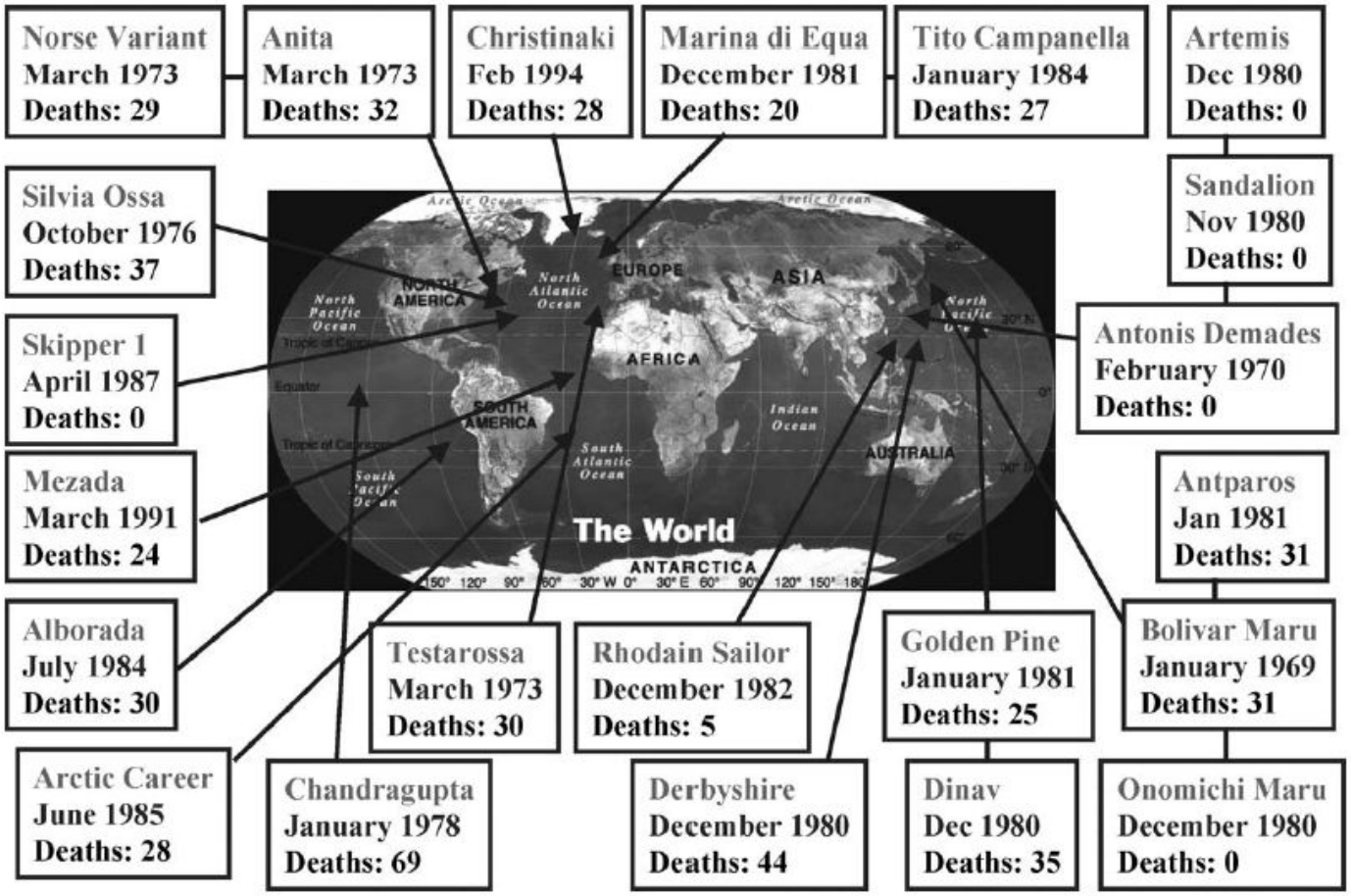

Fig. 1. Statistics of the super-carrier collision with rogue waves for 1968–1994.

Credit: Kharif & Pelinovsky, Eur. Journal of Mechanics B/Fluids **22**, 603 (2003).

Theoretical attempts to explain freak wave formation

... via water surface envelope mode interaction:

PRL 97, 094501 (2006) PHYSICAL REVIEW LETTERS week ending 1 SEPTEMBER 2006

Instability and Evolution of Nonlinearly Interacting Water Waves

P. K. Shukla,[1,2] I. Kourakis,[2] B. Eliasson,[2] M. Marklund,[1] and L. Stenflo[1]
[1]*Centre for Nonlinear Physics, Department of Physics, Umeå University, SE-90187 Umeå, Sweden*
[2]*Institut für Theoretische Physik IV and Centre for Plasma Science and Astrophysics, Fakultät für Physik und Astronomie, Ruhr-Universität Bochum, D-44780 Bochum, Germany*
(Received 16 February 2006; published 30 August 2006)

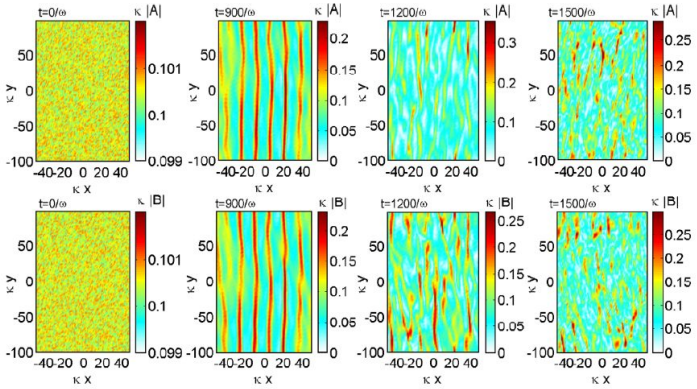

FIG. 4 (color online). The interaction between two waves, initially with equal amplitudes $|A| = |B| = 0.1\kappa^{-1}$ and a propagation angle of $\theta = \pi/8$ relative to the dichotome. Added to the initially homogeneous wave envelopes is a low-amplitude noise of order $10^{-3}/\kappa$ to give a seed to the modulational instability.

EPL, **86** (2009) 24001
doi: 10.1209/0295-5075/86/24001 www.epljournal.org

Evolution of rogue waves in interacting wave systems

A. Grönlund[1,2(a)], B. Eliasson[3] and M. Marklund[3]
[1] *Department of Mathematics, Uppsala University - SE-751 06 Uppsala, Sweden, EU*
[2] *Umeå Plant Science Center, Department of Forest Genetics and Plant Physiology, Swedish University of Agricultural Sciences - SE-901 83 Umeå, Sweden, EU*
[3] *Department of Physics, Umeå University - SE-901 87 Umeå, Sweden, EU*

received 4 December 2008; accepted in final form 16 March 2009

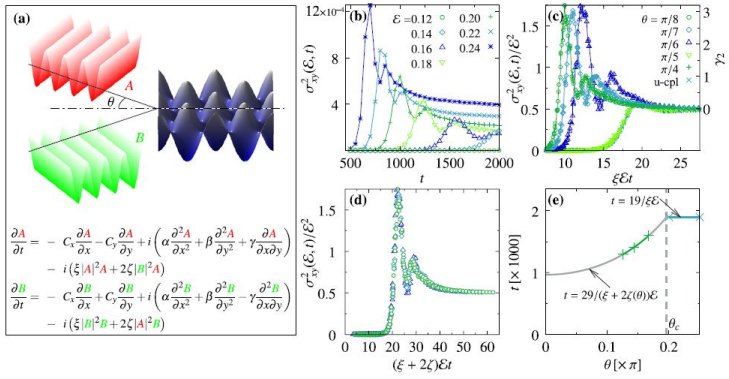

$$\frac{\partial A}{\partial t} = -C_x\frac{\partial A}{\partial x} - C_y\frac{\partial A}{\partial y} + i\left(\alpha\frac{\partial^2 A}{\partial x^2} + \beta\frac{\partial^2 A}{\partial y^2} + \gamma\frac{\partial A}{\partial x\partial y}\right) - i(\xi|A|^2 A + 2\zeta|B|^2 A)$$

$$\frac{\partial B}{\partial t} = -C_x\frac{\partial B}{\partial x} - C_y\frac{\partial B}{\partial y} + i\left(\alpha\frac{\partial^2 B}{\partial x^2} + \beta\frac{\partial^2 B}{\partial y^2} - \gamma\frac{\partial B}{\partial x\partial y}\right) - i(\xi|B|^2 B + 2\zeta|A|^2 B)$$

[Credit: M. Onorato, A.R. Osborne and M. Serio, Phys. Rev. Lett., **96** 014503 (2006);
P. K. Shukla, I. Kourakis, B. Eliasson, M. Marklund and L. Stenflo, Phys. Rev. Lett. **97**, 094501 (2006);
A. Grönlund, B. Eliasson and M. Marklund, EPL, **86** 24001 (2009).]

PRL **106,** 204502 (2011) PHYSICAL REVIEW LETTERS week ending 20 MAY 2011

Rogue Wave Observation in a Water Wave Tank

A. Chabchoub,[1,*] N. P. Hoffmann,[1] and N. Akhmediev[2]

[1]*Mechanics and Ocean Engineering, Hamburg University of Technology, Eißendorfer Straße 42, 21073 Hamburg, Germany*
[2]*Optical Sciences Group, Research School of Physics and Engineering, The Australian National University, Canberra ACT 0200, Australia*

(Received 28 February 2011; published 16 May 2011)

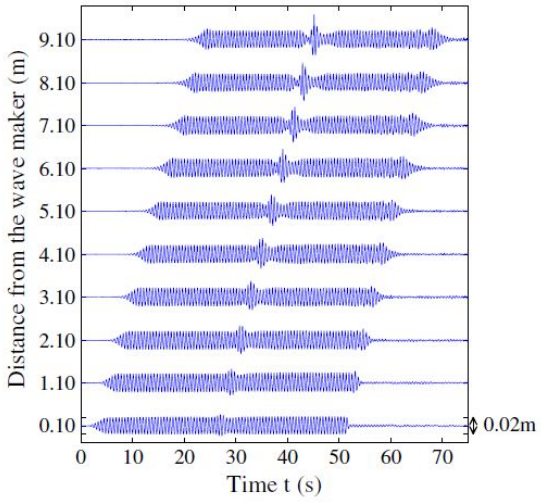

FIG. 3 (color online). Temporal evolution of the water surface height at various distances from the wave maker.

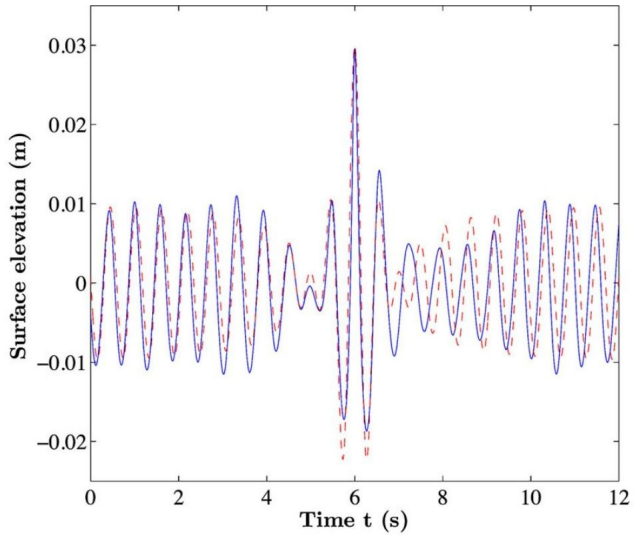

[Credit: A. Chabchoub *et al*, Phys. Rev. Letters **106**, 204502 (2011); (right plot) A. Chabchoub/Hamburg University of Technology (online).]

nature Vol 450|13 December 2007|doi:10.1038/nature06402

LETTERS

Optical rogue waves

D. R. Solli[1], C. Ropers[1,2], P. Koonath[1] & B. Jalali[1]

Recent observations show that the probability of encountering an extremely large rogue wave in the open ocean is much larger than expected from ordinary wave-amplitude statistics[1–3]. Although considerable effort has been directed towards understanding the physics behind these mysterious and potentially destructive events, the complete picture remains uncertain. Furthermore, rogue waves have not yet been observed in other physical systems. Here, we introduce the concept of optical rogue waves, a counterpart of

Although the physics behind rogue waves is still under investigation, observations indicate that they have unusually steep, solitary or tightly grouped profiles, which appear like "walls of water"[10]. These features imply that rogue waves have relatively broadband frequency content compared with normal waves, and also suggest a possible connection with solitons—solitary waves, first observed by J. S. Russell in the nineteenth century, that propagate without spreading in water because of a balance between dispersion and nonlinearity. As

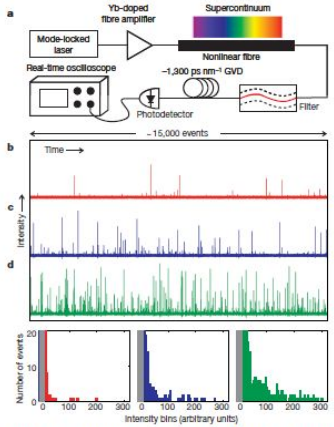

Figure 1 | Experimental observation of optical rogue waves. a, Schematic of experimental apparatus. **b**–**d**, Single-shot time traces containing roughly 15,000 pulses each and associated histograms (bottom of figure: left, **b**; middle, **c**; right, **d**) for average power levels 0.8 μW (red), 3.2 μW (blue) and 12.8 μW (green), respectively. The grey shaded area in each histogram demarcates the noise floor of the measurement process. In each measurement, the vast majority of events (>99.5% for the lowest power) are buried in this low intensity range, and the rogue events reach intensities of at least 30–40 times the average value. These distributions are very different from those encountered in most stochastic processes.

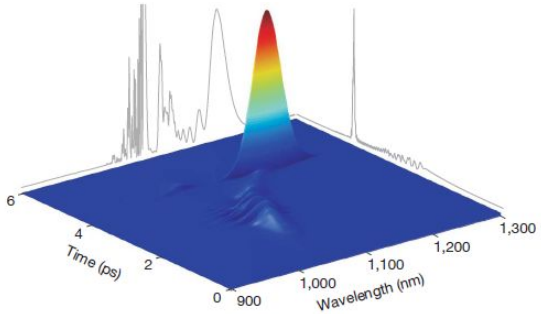

Figure 3 | Time–wavelength profile of an optical rogue wave obtained from a short-time Fourier transform. The optical wave has broad bandwidth and has extremely steep slopes in the time domain compared with the typical events. It appears as a 'wall of light' analogous to the 'wall of water' description of oceanic rogue waves. The rogue wave travels a curved path in time–wavelength space because of the Raman self-frequency shift and group velocity dispersion, separating from non-solitonic fragments and remnants of the seed pulse at shorter wavelengths. The grey traces show the full time structure and spectrum of the rogue wave. The spectrum contains sharp spectral features that are temporally broad and, thus, do not reach large peak power levels and do not appear prominently in the short-time Fourier transform.

Credit: D.R. Solli, C. Ropers, P. Koonath, B. Jalali, Nature **450**, 1054 (2007).

LETTERS
PUBLISHED ONLINE: 22 AUGUST 2010 | DOI: 10.1038/NPHYS1740
nature physics

The Peregrine soliton in nonlinear fibre optics

B. Kibler[1], J. Fatome[1], C. Finot[1], G. Millot[1], F. Dias[2,3], G. Genty[4], N. Akhmediev[5] and J. M. Dudley[6]*

The Peregrine soliton is a localized nonlinear structure predicted to exist over 25 years ago, but not so far experimentally observed in any physical system[1]. It is of fundamental significance because it is localized in both time and space, and because it defines the limit of a wide class of solutions to the nonlinear Schrödinger equation (NLSE). Here, we use an analytic

Our experiments are designed using the breather formalism of ref. 2. With dimensionless field $\psi(\xi,\tau)$, the self-focusing NLSE is:

$$i\frac{\partial\psi}{\partial\xi}+\frac{1}{2}\frac{\partial^2\psi}{\partial\tau^2}+|\psi|^2\psi=0 \qquad (1)$$

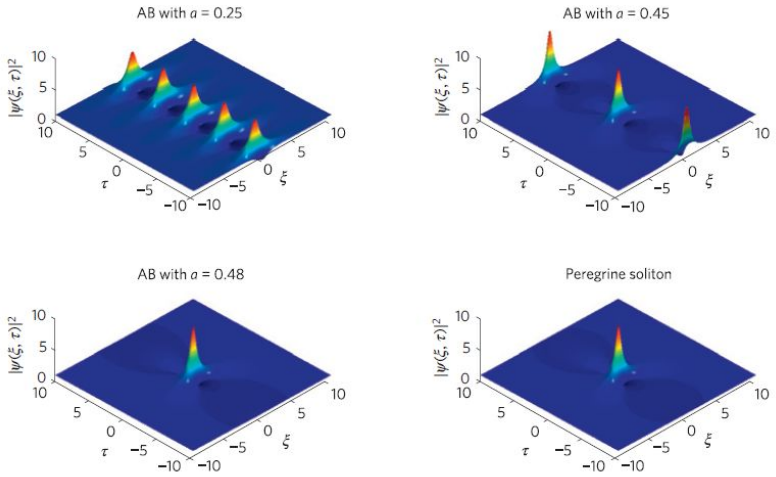

Figure 1 | Plotted Akhmediev breather solutions using equation (2) for modulation parameter $a = 0.25$, $a = 0.45$ and $a = 0.48$, as well as the ideal **Peregrine soliton of equation (3), the limiting case of the Akhmediev breather as $a \to 1/2$.** Maximum temporal compression occurs at normalized distance $\xi = 0$. The differences between the Akhmediev breather (AB) with $a = 0.48$ and the Peregrine soliton can be seen with close inspection of the decay of the peak to the wings; they are shown more clearly in Fig. 2.

[B. Kibler, J. Fatome, C. Finot, G. Millot, F. Dias, G. Genty, N. Akhmediev & JM Dudley, Nat. Phys. **6**, 790 (2010)]

PRL **101,** 065303 (2008) PHYSICAL REVIEW LETTERS week ending 8 AUGUST 2008

Observation of an Inverse Energy Cascade in Developed Acoustic Turbulence in Superfluid Helium

A. N. Ganshin,[1] V. B. Efimov,[1,2] G. V. Kolmakov,[2,1,*] L. P. Mezhov-Deglin,[2] and P. V. E. McClintock[1]
[1]*Department of Physics, Lancaster University, Lancaster, LA1 4YB, United Kingdom*
[2]*Institute of Solid State Physics RAS, Chernogolovka, Moscow region, 142432, Russia*
(Received 20 May 2008; published 8 August 2008)

We report observation of an inverse energy cascade in second sound acoustic turbulence in He II. Its onset occurs above a critical driving energy and it is accompanied by giant waves that constitute an acoustic analogue of the rogue waves that occasionally appear on the surface of the ocean. The theory of the phenomenon is developed and shown to be in good agreement with the experiments.

DOI: 10.1103/PhysRevLett.101.065303 PACS numbers: 67.25.dk, 47.20.Ky, 47.27.−i, 67.25.dt

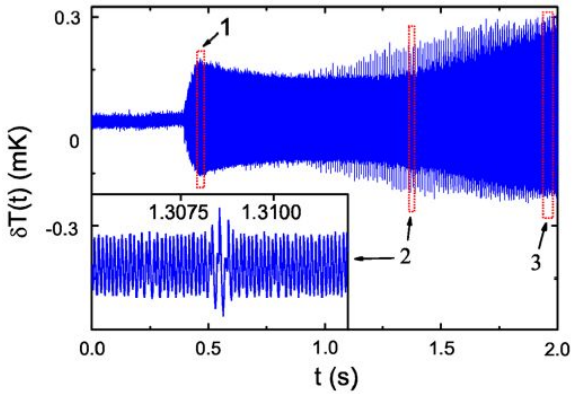

FIG. 3 (color online). Transient evolution of the 2nd sound wave amplitude δT after a steplike shift of the driving frequency to the 96th resonance at time $t = 0.397$ s. Signals in frames 1 and 3 are similar to those obtained in steady-state measurements, Figs. 1(a) and 1(c), respectively. Formation of isolated "rogue" waves is clearly evident. Inset: Example of a rogue wave, enlarged from frame 2.

[A. N. Ganshin *et al*, PRL **101**, 065303 (2008)]

Freak waves everywhere ?

- Rogue wave formation has been investigated in various frameworks, including:
  * oceanic *freak waves* (or *ghost waves*, or rogons, or WANDTs *"Waves that Appear from Nowhere and Disappear without a Trace"*)
    [Akhmediev et al, PLA (2009); Kharif & Pelinovsky, Eur. J. Mech. B/Fluids (2003)]
  * *surface waves* generated in water tank experiments [Chabchoub, PRL (2011)]
  * extreme intensity events (*"rare solitons"*) in *nonlinear optics*
    [Solli et al, Nature (2007); Kibler et al, Nat. Phys. (2010) & Nature/Sci.Rep. (2012)]
  * *errors in data communications* [Savory et al, J. Lightwave Technol. (2006)]
  * *anomalous acoustic turbulence* in superfluid Helium [Ganshin et al, PRL (2008)]
  * rogue cells – forerunners of metastatic cancer [Kaiser, Science (2010)]
  * stock market dynamics: crashes, asset pricing (*Black-Scholes* theory) ...

- Unlike solitary waves (which are propagating excitations which are localized in space), rogue waves may be localized in space *and* in time (*"ghost waves"*).

Analytical models for freak waves

- Breather-type solutions of the *nonlinear Schrödinger (NLS) equation* were proposed by Dysthe & Trulsen (*) as possible analytical models for rogue waves.

Physica Scripta. Vol. T82, 48–52, 1999

Note on Breather Type Solutions of the NLS as Models for Freak-Waves

Kristian B. Dysthe[1] and Karsten Trulsen[2†]

[1]Department of Mathematics, University of Bergen, Johs.Brunsgt.12, 5008 Bergen, Norway
[2]Instituto Pluridisciplinar, Universidad Complutense de Madrid, Paseo Juan XXIII 1, E–28040 Madrid, Spain,

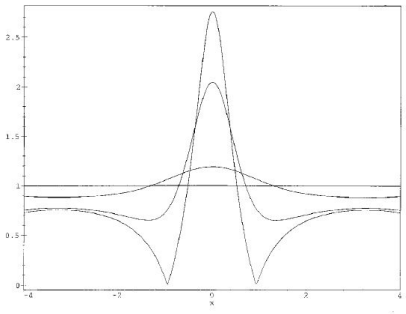

Fig. 1. The Akhmediev solution (6) for $\varphi = 0.5$. The envelope $|q|$ is shown as a function of x and t in (a), and the time evolution of one period $2\pi/p$ of the spatial profile is shown in (b).

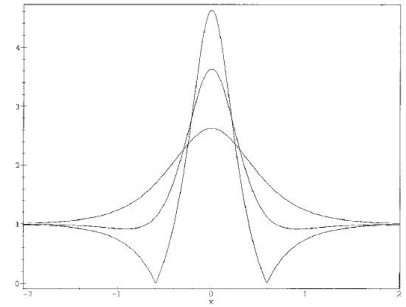

Fig. 2. The Ma-breather (13) for $\varphi = 1.2$. The envelope $|q|$ is shown as a function of x and t in (a), and the spacial profile of the envelope through a period $2\pi/\Omega$ is shown in (b).

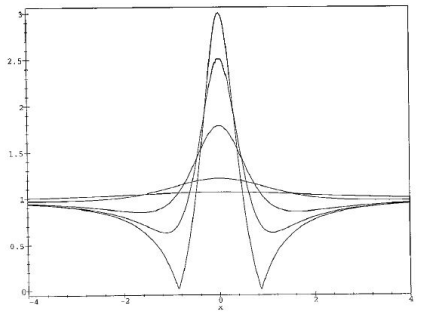

Fig. 3. The Peregrine solution (8). The envelope $|q|$ is shown as a function of x and t in (a), and the time evolution of the spacial profile of the envelope is shown in (b).

[(*) K.B. Dysthe and K. Trulsen, Phys. Scripta T**82**, 48 (1999)]

What about ... freak waves in plasmas? (1)

- The *freak wave* paradigm was employed in plasmas as a possible mechanism for magnetic hole generation by *Michael Ruderman* (*), who considered the generation of Alfvén type freak waves by adopting a *Derivative Nonlinear Schrödinger (DNLS)* equation model.

Eur. Phys. J. Special Topics **185**, 57–66 (2010)

DOI: 10.1140/epjst/e2010-01238-7

THE EUROPEAN PHYSICAL JOURNAL SPECIAL TOPICS

Regular Article

Freak waves in laboratory and space plasmas

Freak waves in plasmas

M.S. Ruderman[a]

School of Mathematics and Statistics, University of Sheffield, Hounsfield Road, Hicks Building, Sheffield S3 7RH, UK

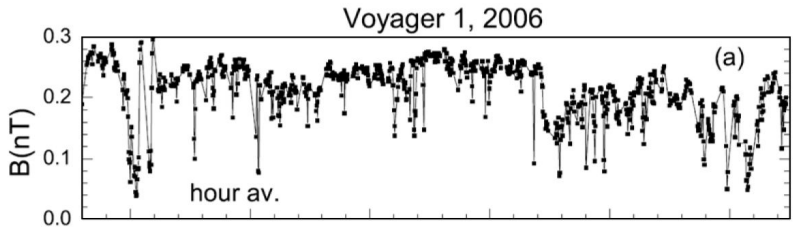

Fig. 1. Voyager 1 observations of hour averages of the magnetic field strength B in the heliosheath. The magnetic field magnitude shows many spike-like dips that are too narrow to be resolved in the hour average. Figure taken from Ref. [10].

[(*) MS Ruderman, Eur. Phys. J. Special Topics **185**, 57 (2010)]

Freak waves in plasmas (2)

Rogue waves have been considered recently in various plasma contexts:

- *Alfvén-type rogue waves* [Shukla et al, Physics Letters A (2012)]
- *Langmuir rogue waves in electron-positron plasmas* [Moslem, PoP 2011]
- *Electrostatic waves in e-p-i plasmas* [El-Awady & Moslem, Phys. Plasmas 2011; El-Labany *et al*, Astrophys. Space Sci. 2012]
- *Dusty plasmas* [Abdelsalam, *et al*, Phys. Plasmas 2011; Moslem *et al*, PRE 2011]
- *Surface plasma waves* [Moslem, Shukla and Eliasson, Europhys. Lett. 2011].
- Most of these studies have relied on a phenomenological analogy between rogue waves and large amplitude solutions of nonlinear model PDEs, e.g. KdV/mKdV or NLS equations (families).

iopscience.iop.org/2040-8986/labtalk-article/53714

IOPscience Journals Books Login Search Article lookup

Journal of Optics

Email alert RSS feed

Monster waves in a laser beam: myth or reality?

How can ultra-strong electromagnetic excitations be formed during the interaction of a laser beam with a plasma?

The unexpected occurrence of a huge water-wall (generally termed a rogue wave, or freak wave) has been a nightmare for seafarers (Onorato *et al* 2001 *Phys. Rev. Lett.* **86** 5831; Shukla *et al* 2006 *Phys. Rev. Lett.* **97** 094501) and a fascinating subject of research for nonlinear physicists (Akhmediev *et al* 2009 *Phys. Rev.* A **80** 043818). The amplitude of these giant waves is often reported to exceed twice or thrice the average height of surrounding waves (background turbulence), a fact suggesting a nonlinear description should be adopted as a model. This is a hot topic of current research, both in ocean physics and in other areas, including nonlinear optics, photonics and, more recently, in plasma physics. A better understanding of the formation of such destructive waves in the ocean would lead to the possibility of predicting, or even suppressing their occurrence. On the other hand, in nonlinear optics they can be used to generate high amplitude pulses when required. Significant research effort is being invested in elucidating the conditions for such excitations to occur, and in identifying their spatial and temporal characteristics.

In charged matter (plasma), by now recognized as the fourth state of matter and as the main

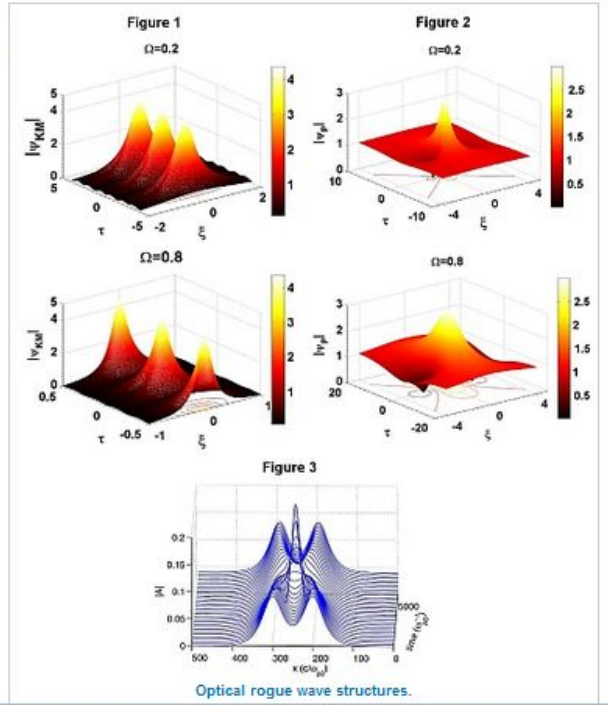

Optical rogue wave structures.

Related links

Electromagnetic rogue waves in beam–plasma interactions

Special issue on Optical Rogue Waves

Most recent | Most read

Enhanced transmission under evanescent incidence
Apr 25, 2014

Low refractive index sensing
Apr 25, 2014

Simultaneous measurement of refractive index and thickness
Apr 22, 2014

More LabTalk

[*Electromagnetic Rogue Waves in Beam-Plasma Interactions*, G.P. Veldes, J. Borhanian, M. McKerr, V. Saxena, D.J. Frantzeskakis and I. Kourakis, *J. Optics* **15** (Special issue on Optical Rogue Waves), 064003 (2013);

IoP LabTalk article (online, 2013): *Monster waves in a laser beam: myth or reality?*]

IOP Publishing
Plasma Phys. Control. Fusion 56 (2014) 035007 (17pp)
Plasma Physics and Controlled Fusion
doi:10.1088/0741-3335/56/3/035007

Freak waves and electrostatic wavepacket modulation in a quantum electron–positron–ion plasma

M McKerr[1], I Kourakis[1] and F Haas[2]

[1] Centre for Plasma Physics, School of Mathematics and Physics, Queen's University Belfast, BT7 1NN Belfast, Northern Ireland, UK
[2] Departamento de Física, Universidade Federal do Paraná, 81531-990, Curitiba, Paraná, Brazil

Received 2 July 2013, revised 8 January 2014
Accepted for publication 13 January 2014
Published 5 February 2014

Abstract
The occurrence of rogue waves (freak waves) associated with electrostatic wavepacket propagation in a quantum electron–positron–ion plasma is investigated from first principles. Electrons and positrons follow a Fermi–Dirac distribution, while the ions are subject to a quantum (Fermi) pressure. A fluid model is proposed and analyzed via a multiscale technique. The evolution of the wave envelope is shown to be described by a nonlinear Schrödinger equation (NLSE). Criteria for modulational instability are obtained in terms of the intrinsic plasma parameters. Analytical solutions of the NLSE in the form of envelope solitons (of the bright or dark type) and localized breathers are reviewed. The characteristics of exact solutions in the form of the Peregrine soliton, the Akhmediev breather and the Kuznetsov–Ma breather are proposed as candidate functions for rogue waves (freak waves) within the model. The characteristics of the latter and their dependence on relevant parameters (positron concentration and temperature) are investigated.

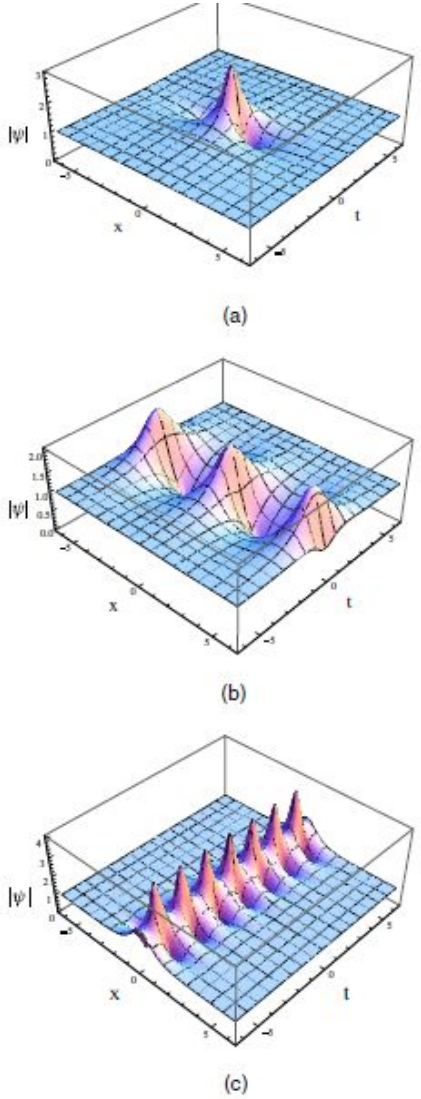

Figure 16. The three waveforms, as presented in the text, are here plotted against x and t: (a) Peregrine's 'Soliton', (b) Akhmediev's breather and (c) Ma's breather. The spatial and temporal behavior of each is clearly displayed. $P = Q = \varphi = 1$.

Freak waves observed in plasma experiments?

– Random events – hard to observe in the laboratory!

– First experiment on negative-ion plasmas (NIPs):

PRL 107, 255005 (2011) PHYSICAL REVIEW LETTERS week ending 16 DECEMBER 2011

Observation of Peregrine Solitons in a Multicomponent Plasma with Negative Ions

H. Bailung,[1] S. K. Sharma,[1] and Y. Nakamura[1,2]

[1]*Plasma Physics Laboratory, Physical Sciences Division, Institute of Advanced Study in Science and Technology, Paschim Boragaon, Guwahati-35, India*

[2]*On leave from Yokohama National University, Yokohama, Japan*

(Received 29 July 2011; published 16 December 2011)

The experimental observation of Peregrine solitons in a multicomponent plasma with the critical concentration of negative ions is reported. A slowly amplitude modulated perturbation undergoes self-modulation and gives rise to a high amplitude localized pulse. The measured amplitude of the Peregrine soliton is 3 times the nearby carrier wave amplitude, which agrees with the theory. The numerical solution of the nonlinear Schrödinger equation is compared with the experimental results.

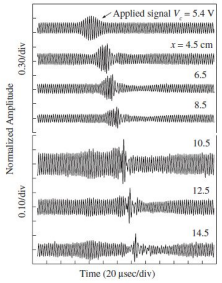

FIG. 2. Observed signals of the electron density perturbation at different probe positions from the separation grid. The top trace is the applied signal with carrier and modulation frequencies 350 and 31 kHz, respectively. Peak to peak amplitude of the applied carrier wave (V_c) is fixed at 5.4 V. Signals observed at 10.5 to 14.5 cm are shown with different amplitude scale (0.10/div) for better resolution.

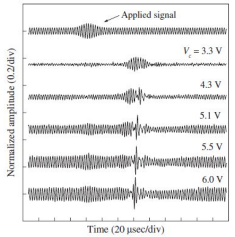

FIG. 3. Signals recorded for different excitation amplitudes of the carrier wave. The probe is fixed at 13.6 cm from the separation grid. Top trace represents the applied signal with carrier and modulation frequencies 350 and 31 kHz, respectively.

[9]. The slight shift in the phase of the carrier part with theory is probably due to the presence of pseudowave in front of the solitons [15]. However, detailed investigation is necessary for confirmation. We analyzed the wave signals

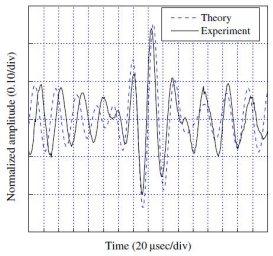

FIG. 4 (color online). Comparison of the time series signal (solid line) observed at 13.6 cm with the theoretical Peregrine soliton (dashed line) obtained by using Eq. (3). The applied carrier and modulation frequencies are 350 and 31 kHz, respectively. $V_c = 5.9$ V. The parameters used for numerical calculations are $\omega = 0.7\omega_{pi}$, ($\omega_{pi} = 492$ kHz), $k = 0.74k_D$, $k_D = 1/\lambda_D = 20.0$ cm^{-1}.

– Second experiment (in dusty plasmas) announced Feb. 2016!

nature physics

LETTERS

PUBLISHED ONLINE: 29 FEBRUARY 2016 | DOI: 10.1038/NPHYS3669

Generation of acoustic rogue waves in dusty plasmas through three-dimensional particle focusing by distorted waveforms

Ya-Yi Tsai, Jun-Yi Tsai and Lin I*

Rogue waves—rare uncertainly emerging localized events with large amplitudes—have been experimentally observed in many nonlinear wave phenomena, such as water waves[1–6], optical waves[7,8], second sound in superfluid He II (ref. 9) and ion acoustic waves in plasmas[10]. Past studies have mainly focused on one-dimensional (1D) wave behaviour through modulation instabilities[1,3–5,7,11], and to a lesser extent on higher-dimensional behaviour[5,6,8,11,12]. The question whether rogue waves also exist in nonlinear 3D acoustic-type plasma waves, the kinetic origin of their formation and their correlation with surrounding 3D waveforms are unexplored fundamental issues. Here we report the direct experimental observation of dust acoustic rogue waves in dusty plasmas and construct a picture of 3D particle focusing by the surrounding tilted and ruptured wave crests, associated with the higher probability of low-amplitude holes for rogue-wave generation.

Modulation instability (MI) which makes the wave modulation envelope unstable has been well accepted as a mechanism for rogue-wave or envelope soliton generation in systems governed by nonlinear equations, such as the nonlinear Landau–Ginzburg or Schrödinger equations[1,3–5,7,11,12]. On the other hand, recent studies in nonlinear water, chemical and dust acoustic waves, also demonstrated that MI causes 3D waveform undulation, rupture (refs 15,16,19,29) are the few examples giving experimental evidence of the ubiquitous behaviour in many other nonlinear media. The advantages of direct video imaging large-area dust density evolution and tracking individual particle motion at the discrete level also make it a good platform to construct an Eulerian–Lagrangian picture as a means of understanding dynamics in nonlinear density wave systems[18,19,28]. Nevertheless, RWEs have been demonstrated theoretically only in 1D dust acoustic waves[22].

The experiment is conducted in a cylindrical radiofrequency (rf) dusty-plasma system, as sketched in Fig. 1a (also see Methods)[16]. Figure 1b shows a typical temporal waveform of n_d, the normalized local dust density, in the disordered state of the self-excited downward propagating DAW. The irregular amplitude modulation evidences MI and causes the broadening of the fundamental and higher harmonic peaks in its power spectrum (Fig. 1c).

Figure 1d shows the histogram of the wave height H measured from 12,000 images. As commonly used for oceanic RWEs, the stretched tail beyond $2H_s$ signifies RWEs, where H_s (=2) is the significant wave height, defined as the average of the highest third of all wave heights[1,2]. Figure 1e shows the highly localized and randomly distributed RWEs in the xyt space over 120 wave cycles. The averaged wavelength λ and wave period τ_0 are 1 mm and 32 ms, respectively.

[Ya-Yi Tsai, Jun-Yi Tsai and Lin I, Nature (Physics) (2016) - DOI: 10.1038/NPHYS3669 .]

Intro #2: Nonlinear Amplitude Modulation (prerequisites)

- Harmonic variation of the amplitude of a plasma wavepacket
- Amplitude not constant, may vary weakly in space and time
- Ubiquitous nonlinear mechanism, associated with
  * *secondary harmonic generation*
  * *modulational instability*
  * *envelope solitons*: localized forms with periodic internal structure
  * *Freak waves???*
- ***Energy localization***: lumps of energy are formed and propagate in the plasma; dynamics to be harnessed for applications

Intro: Prerequisites *(continued)*

The *amplitude* of a harmonic wave may vary in space and time:

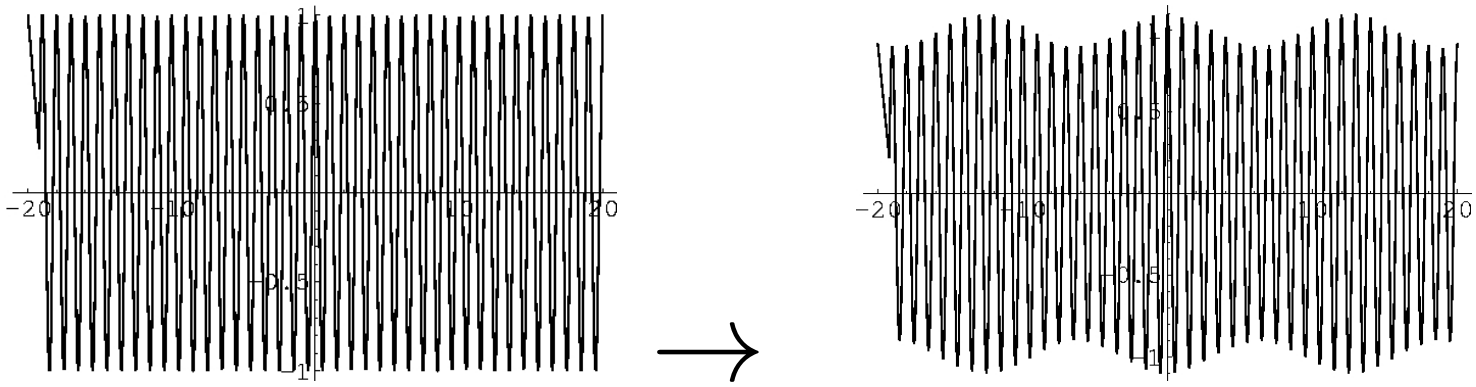

Intro: Prerequisites *(continued)*

The *amplitude* of a harmonic wave may vary in space and time:

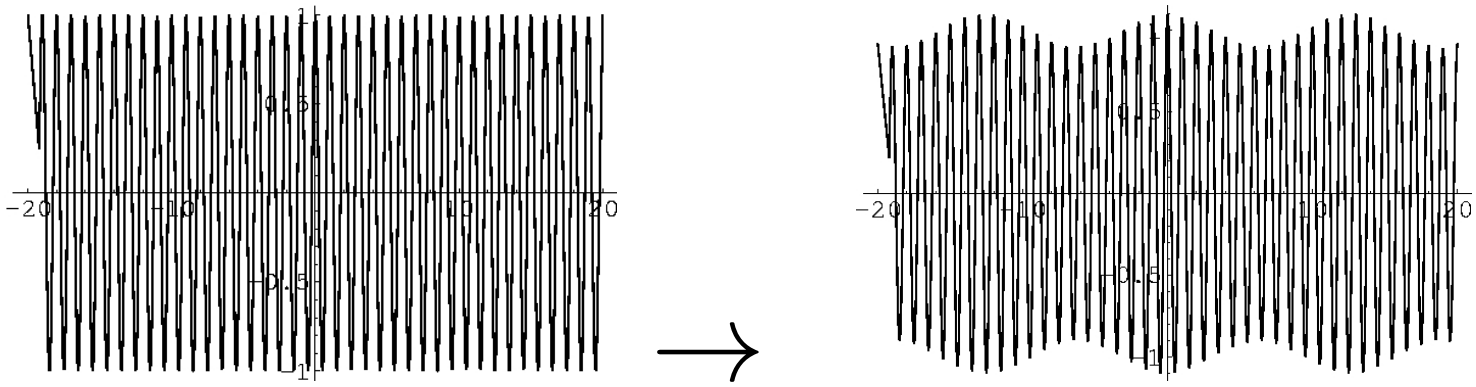

This *modulation* (due to nonlinearity) may be *strong* enough to lead to wave *collapse* (modulational instability) or ...

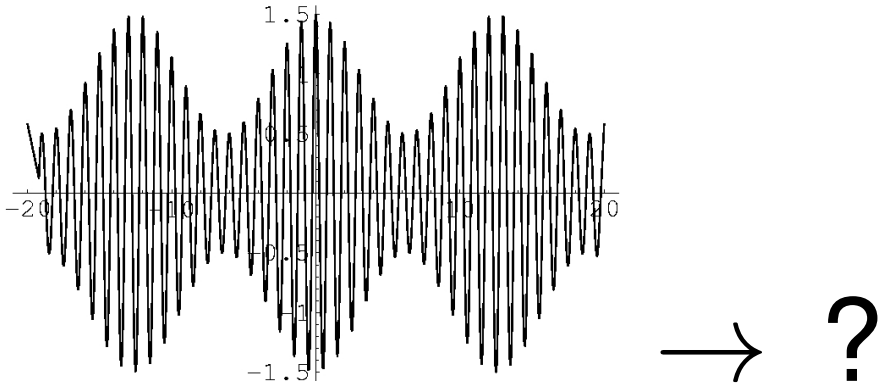

?

Intro: Prerequisites *(continued)*

The *amplitude* of a harmonic wave may vary in space and time:

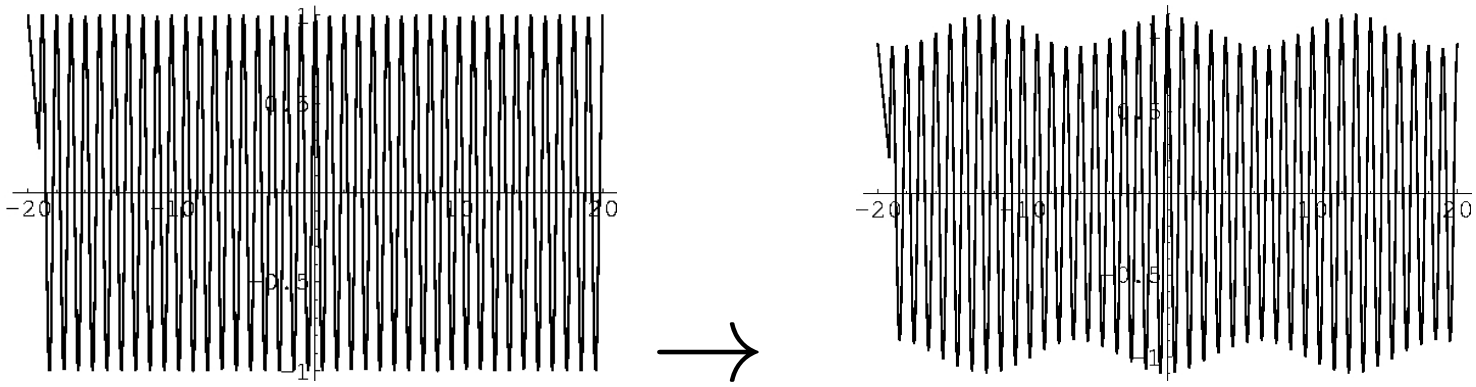

This *modulation* (due to nonlinearity) may be *strong* enough to lead to wave *collapse* (modulational instability) or to the formation of *envelope solitons*:

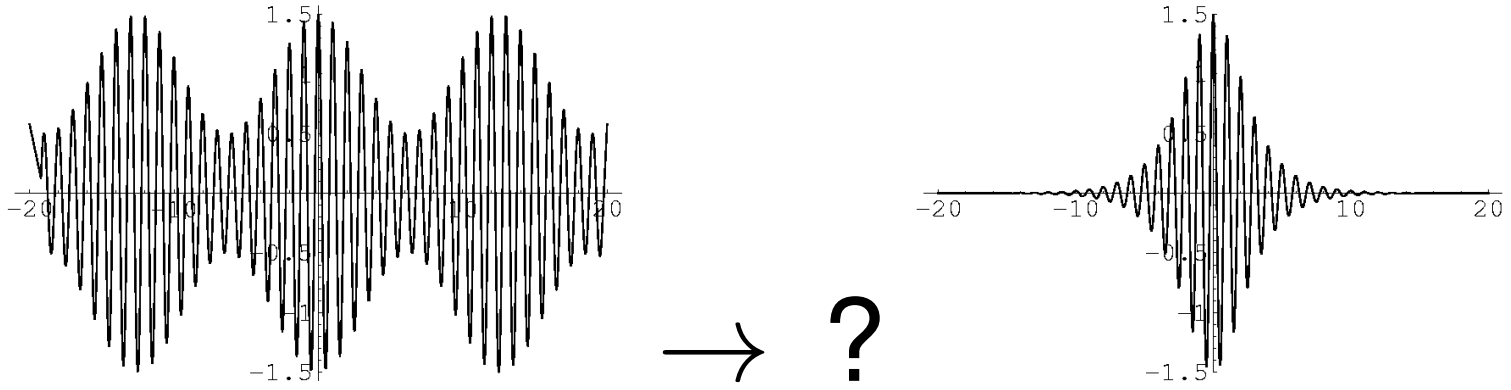

Modulated structures occur widely, e.g. in EM field measurements in the magnetosphere, ...

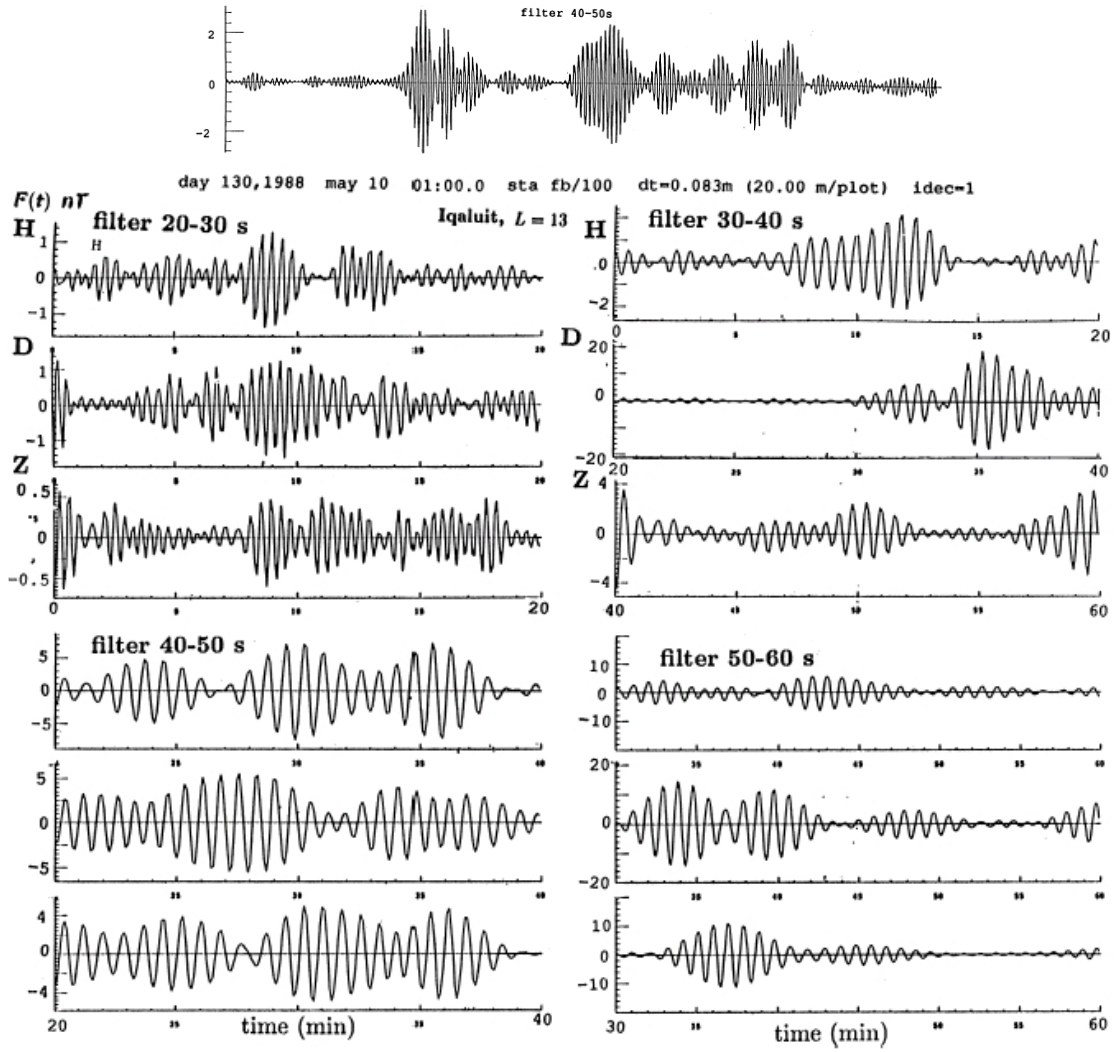

(from: [Ya. Alpert, Phys. Reports **339**, 323 (2001)])

Part 2: Focus on *Negative-ion plasmas (NIP)*

Negative ion plasmas (NIP) occur in:

- The Earth's ionosphere [Yu. I. Portnyagin, et.al, Adv. Space Res. 11, 89 (1991)]
- Cometary Comae [P. H. Chaizy,et.al. , Nature (London) 349, 393 (1991)]
- Titan's Atmosphere [A. J. Coates *et al*, GRL **34** (2007)]
- Plasma Processing Reactors [RA Gottscho & CE Gaebe, IEEE Trans. Plasma Sci. **14**, 92 (1986)]
- Neutral Beam Sources [M Bacal and GW Hamilton, PRL **42**, 1538 (1979)]
- Low-Temperature Laboratory Experiments [A. Weingarten *et al*, PRL **87**, 115004 (2001)]
- Experiments on freak waves in NIP: H Bailung, SK Sharma and Y Nakamura, PRL **107**, 255005 (2011); SK Sharma and H Bailung, J. Geophys. Res. **118**, 919 (2013).
- Theoretical investigations: M Saito et al, J. Phys. Soc. Jpn., **53**, 2304 (1984); MS Ruderman, T Talipova and E Pelinovsky, J. Plasma Phys., 74, 639 (2008); SK Sharma & H Bailung, J. Geophys. Res. **118**, 919 (2013).

Inspiration: Michael Ruderman *et al*, JPP 74, 639 (2008)

M Ruderman *et al* (2008) considered the modulation instability mechanism in negative-ion plasmas, by using a Gardner equation approach:

J. Plasma Physics (2008), *vol.* 74, *part* 5, *pp.* 639–656.
doi:10.1017/S0022377808007150 Printed in the United Kingdom

Dynamics of modulationally unstable ion-acoustic wavepackets in plasmas with negative ions

MICHAEL S. RUDERMAN[1], TATYANA TALIPOVA[2] and EFIM PELINOVSKY[2]

[1] Department of Applied Mathematics, University of Sheffield, Hicks Building, Hounsfield Road, Sheffield S3 7RH, UK
(m.s.ruderman@sheffield.ac.uk)

Inspiration: Michael Ruderman *et al*, JPP 74, 639 (2008)

2 Modulationally unstable ion-acoustic waves in plasmas with negative ions

2.1 Gardner equation for nonlinear waves

Nonlinear ion-acoustic waves in plasmas have been studied for a very long period of time. It was shown that the Korteweg-de Vries (KdV) equation can be used to describe waves with moderate amplitudes [16–18]. The KdV-type ion-acoustic solitons in plasmas consisting of electrons and positive ions were then studied experimentally [19–23].

The behaviour of ion-acoustic waves becomes mode complicated when the plasma contains not only positive but also negative ions. When the concentration of negative ions is equal to the critical value, the coefficient at the nonlinear term in the KdV equation is equal to zero, which implies that the cubic non-linearity has to be takes into account. As a result, nonlinear ion-acoustic waves in plasmas with the critical concentration of negative ions are described by the modified Korteweg-de Vries (mKdV) equation [24–28]. The mKdV solutions were also observed in the experiment [29].

When the negative ion concentration is not exactly equal to the critical value, but close to it, both the quadratic and cubic non-linearity has to be taken into account. In that case the dynamics of nonlinear ion-acoustic waves is described by the Gardner equation [30,31],

$$\frac{\partial \psi}{\partial \tau} - a\psi \frac{\partial \psi}{\partial \xi} + g\psi^2 \frac{\partial \psi}{\partial \xi} + \chi \frac{\partial^3 \psi}{\partial \xi^3} = 0. \qquad (1)$$

The fineprint: a number of hypotheses underlies the treatment by Ruderman *et al*:

- NIP ***near-critical concentration***, so that the quadratic nonlinearity term in the KdV equation is *nearly zero*;
- Gardner equation, i.e.
  - ***small-amplitude*** ($\phi \ll kT_e/m$),
  - ***small-wavenumber*** $k \ll \lambda_D^{-1}$ (long wavelength $\lambda \gg \lambda_D$),
  - ***weakly-superacoustic*** ($v_{sol} \simeq c_s + \epsilon\delta v$) approximation.
- Questions:
  - Are the above requirements important?
  - Could freak waves be generated in NIPs in other conditions?
    And, in particular, in more general (non"critical") plasma configurations?

[Source(s): MS Ruderman, T Talipova and E Pelinovsky, JPP **74**, 639 (2008); *ibid*, in EPJD **185** (2010)]

Part 3: Analytical framework – 3-fluid model

- We consider a three component collisionless unmagnetized plasma consisting of:
  - ⋆ electrons (mass m_e, charge e), thermalized (inertialess)
  - ⋆ positive ions (mass m_p, charge $q_p = Z_p e$)
  - ⋆ negative ions (mass m_n, charge $q_n = -Z_n e$)

- Electrostatic approximation + three-ion fluid model + Poisson's equation:

$$\partial_t n_p + \nabla(n_p u_p) = 0, \tag{1}$$

$$\partial_t u_p + u_p \nabla(u_p) = -\frac{q_p}{m_p}\nabla\phi, \tag{2}$$

$$\partial_t n_n + \nabla(n_n u_n) = 0, \tag{3}$$

$$\partial_t u_n + u_n \nabla(u_n) = -\frac{q_n}{m_n}\nabla\phi, \tag{4}$$

$$\nabla^2\phi = 4\pi[e n_e - q_p n_p - q_n n_n], \tag{5}$$

- Quasi-neutrality assumption: at equilibrium, $n_{e0}e - q_n n_{n0} - q_p n_{p0} = 0$.

- The model equations are cast in a dimensionless form as

$$\partial_t n_p + \nabla(n_p u_p) = 0, \tag{6}$$
$$\partial_t u_p + u_p \nabla(u_p) = -\nabla\phi, \tag{7}$$
$$\partial_t n_n + \nabla(n_n u_n) = 0, \tag{8}$$
$$\partial_t u_n + u_n \nabla(u_n) = \delta \nabla\phi, \tag{9}$$
$$\nabla^2\phi = -n_p + \beta\, n_n + (1-\beta)\, f(\phi)\,, \tag{10}$$

where $f(\phi) = \exp\left(\frac{e\phi}{k_B T_e}\right) \simeq 1 + c_1\phi + c_2\phi^2 + c_3\phi^3$ (Maxwellian assumption).

- T_e is the electron temperature; $c_1 = 2c_2 = 6c_3 = 1$.

- Dimensionless parameters: $\beta = \frac{Z_n n_{0n}}{Z_p n_{0p}}\,, \quad \delta = \frac{Z_n/m_n}{Z_p/m_p}\,.$

- Scaling: $T_0 = \omega_{p,+}^{-1} = (4\pi e^2 n_{p,0} Z_p^2/m_p)^{-1/2}\,, \quad \phi_0 = k_B T_e/e$
  $\lambda_{D,+} = \left(k_B T_e/4\pi Z_p e^2 n_{po}\right)^{1/2}\,, \quad C_s = V_0 = (Z_p k_B T_e/m_p)^{1/2}\,.$

Multiscale perturbative technique for envelope dynamics

- Following the multiple scales (reductive perturbation) technique of Taniuti and coworkers (JMP & JPSJ 1969), we consider the stretched variables

$$X_n = \epsilon^n x \; ; \quad T_n = \epsilon^n t \; ; \qquad n = 0, 1, 2, ...$$

- We define the state vector $\mathbf{S} = (n_p, u_p; n_n, u_n; \phi)$, and
- proceed by expanding near the equilibrium state $\mathbf{S}^{(0)} = (1, 0, 0, 0, 0)$ as

$$\mathbf{S} = \mathbf{S}^{(0)} + \sum_{n=-\infty}^{n} \epsilon^n \mathbf{S}^{(n)}$$

where

$$\mathbf{S}^{(n)} = \sum_{l=-n}^{n} \mathbf{S}_l^{(n)} \, e^{il(kx-\omega t)}$$

denotes the amplitude of the $n-$th order contribution, as a series of the $l-$th harmonic amplitude(s) $\mathbf{S}_{(l)}^{(n)} = \mathbf{S}_{(l)}^{(n)}(X_j, T_j)$ (*slow*, for $j \geq 1$).

Perturbative scheme – results

- *Dispersion relation*:

$$\omega^2 = \frac{(1+\delta\beta)k^2}{k^2+(1-\beta)}$$

Or, restoring dimensions,

$$\omega^2 = \frac{\omega_{p,p}^2\,(1+\delta\beta)\,(k\lambda_{D,p})^2}{(k\lambda_{D,p})^2+(1-\beta)}$$

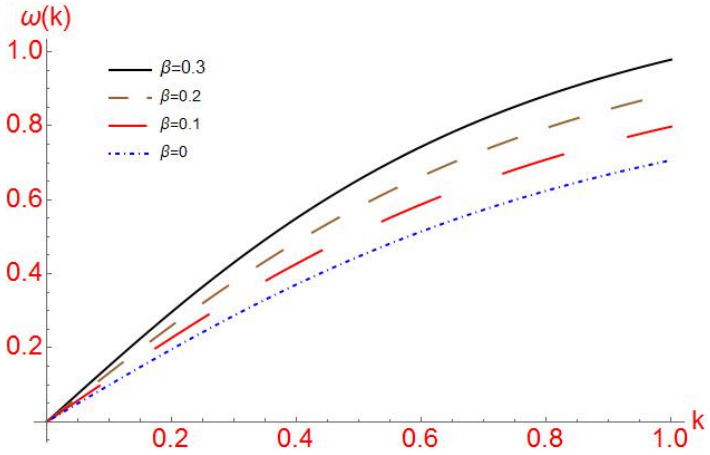

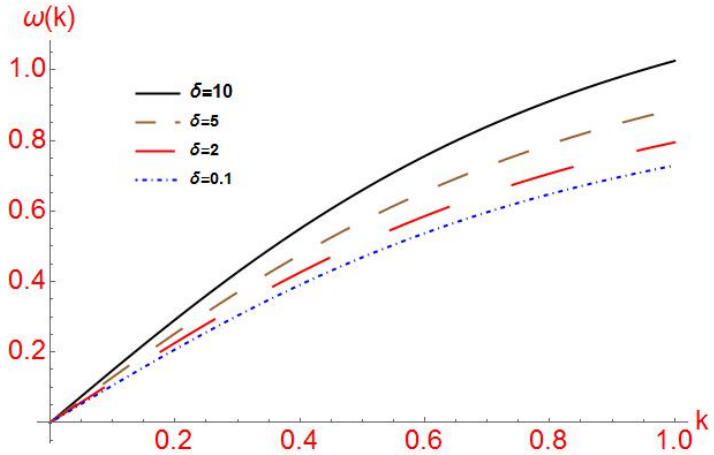

Modified charge (Debye) screening length versus β:

$\lambda_{D,p}^{(\beta)} = 1/\sqrt{(1-\beta)}\,\lambda_{D,p}\,.$

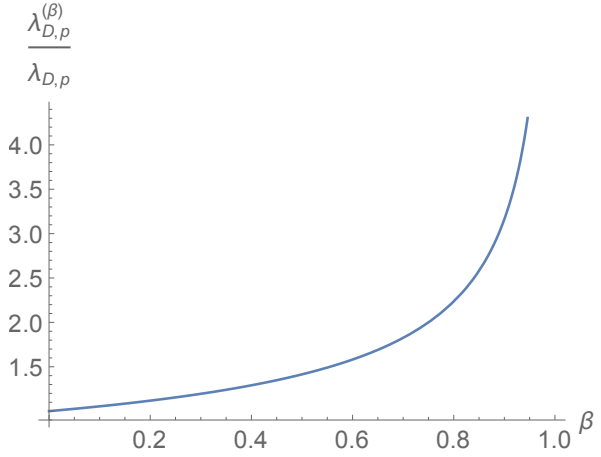

Modified phase speed: $v_{ph} = \frac{(1-\beta)\sqrt{1+\beta\delta}}{[k^2+(1-\beta)]^{3/2}} \simeq \left(\frac{1+\beta\delta}{1-\beta}\right)^{1/2} \qquad (\text{for } k \ll 1).$

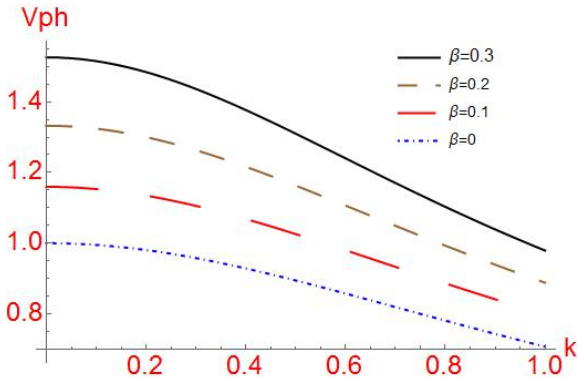

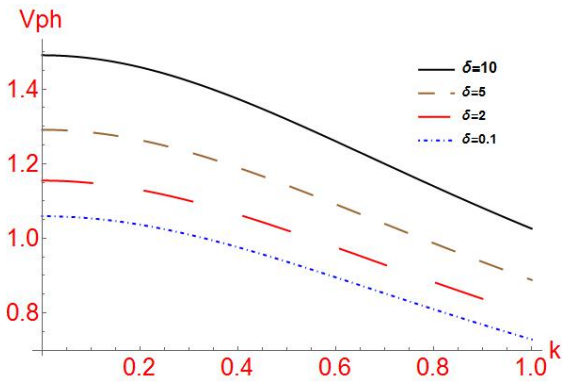

- In order $\sim \epsilon^2$:

$$\partial_1 \phi_1^{(1)} + v_g \nabla_1 \phi_1^{(1)} = 0.$$

- The envelope $\phi_1^{(1)} = \phi_1^{(1)}(X_1 - v_g T_1)$ moves at the *group velocity*:

$$v_g = \frac{d\omega}{dk} = \frac{(1-\beta)(1+\delta\beta)^{\frac{1}{2}}}{[k^2 + (1-\beta)]^{\frac{3}{2}}}.$$

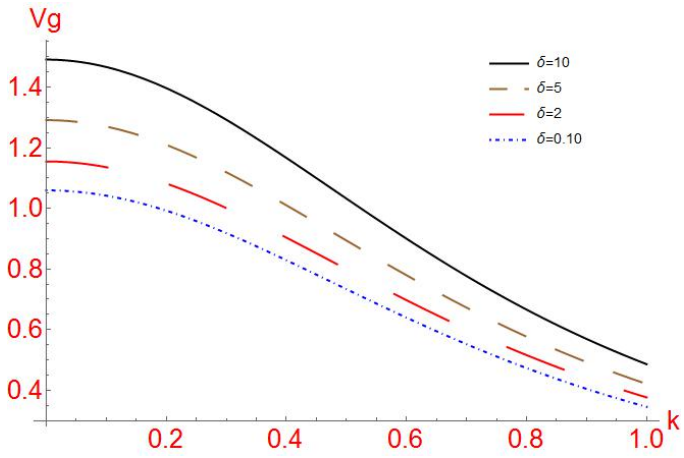

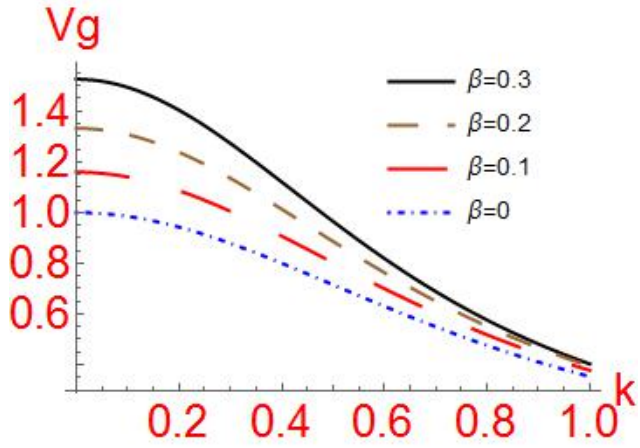

- Increasing the charge-density and mass ratios makes ion acoustic structures faster, i.e., increases the group velocity.

NLS equation for the vector potential (amplitude) $A_1^{(1)}$

- In order $\sim \epsilon^3$:
- This analytical requirement can be expressed in the form

$$i\left(\frac{\partial A_1^{(1)}}{\partial T_2}+v_g\frac{\partial A_1^{(1)}}{\partial X_2}\right)+P\frac{\partial^2 A_1^{(1)}}{\partial X_1^2}+Q\,|A_1^{(1)}|^2A_1^{(1)}=0$$

- Dispersion coefficient P : $P=\frac{1}{2}\left[\frac{3v_g^2}{\omega}+\frac{\omega}{k^2}-\frac{4v_g}{k}-\frac{\omega^3}{\gamma(1+\delta\beta)k^2}\right]$
- Nonlinearity coefficient Q:

$$Q=\frac{(1-\beta)\omega^3}{2(1+\delta\beta)k^2}\left[2c_2(A+B)+3c_3\right]-\frac{(1-\delta^2\beta)}{(1+\delta\beta)}\left[\frac{Bk}{v_g}+\frac{B\omega}{2v_g^2}+\frac{3Ak^2}{2\omega}\right]$$
$$-\frac{(1+\delta^3\beta)}{(1+\delta\beta)}\left[\frac{k^2}{2\omega v_g^2}+\frac{2k^3}{\omega^2 v_g}+\frac{5k^4}{4\omega^3}\right].$$

Modulational (in)stability analysis

- *Perturb* the amplitude by setting: $\hat{\psi} = \hat{\psi}_0 + \epsilon\,\hat{\psi}_{1,0}\cos\left(\tilde{k}\zeta - \tilde{\omega}\tau\right)$
- We obtain the *(perturbation)* dispersion relation:

$$\tilde{\omega}^2 = P^2\,\tilde{k}^2\left(\tilde{k}^2 - 2\,\frac{Q}{P}\,|\hat{\psi}_{1,0}|^2\right).$$

- If $PQ < 0$: the amplitude ψ is *stable* to external perturbations:

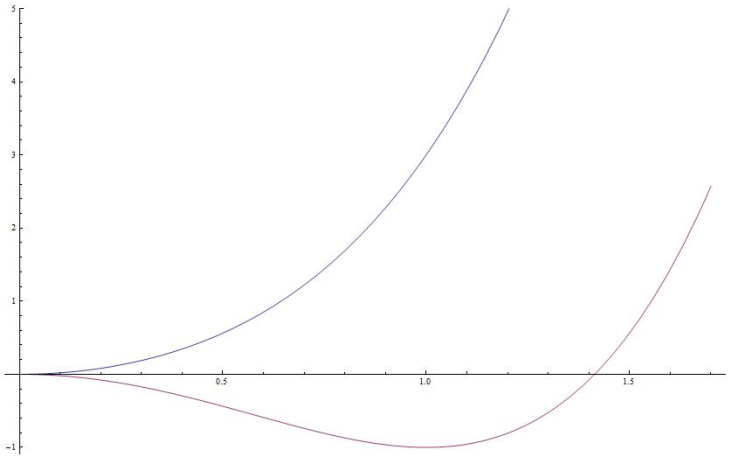

Modulational (in)stability analysis (continued...)

- If $PQ > 0$: the amplitude ψ is *unstable* for $\tilde{k} < \sqrt{2\,\frac{Q}{P}}\,|\psi_{1,0}|$.

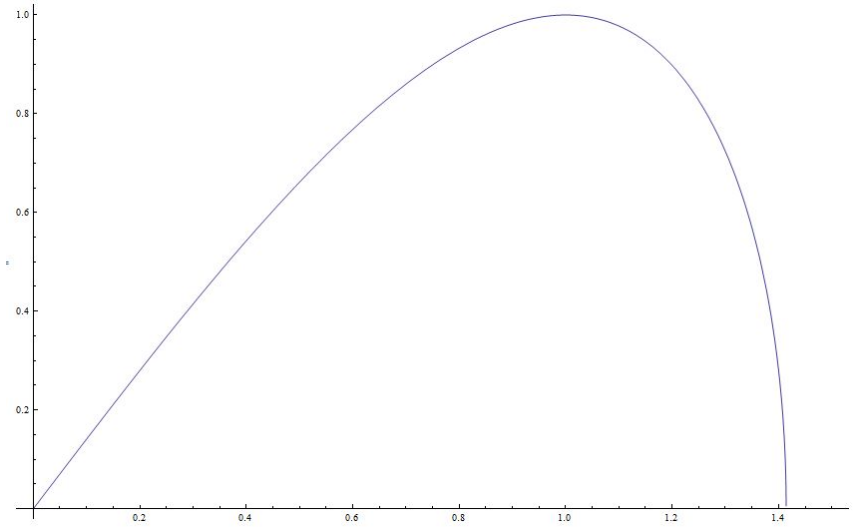

- Maximum (instability) growth rate: $\sigma = Q|\psi_{1,0}|^2$, occurs at $\tilde{k}_m < \sqrt{\frac{Q}{P}}\,|\psi_{1,0}|$

- Instability occurs in the "window": $0 < \tilde{k} < \sqrt{2\,\frac{Q}{P}}\,|\psi_{1,0}|$.

- The wave may either "blow up", or localize its energy towards the formation of (envelope) solitons.

Localized envelope excitations (solitons)

- The NLSE accepts various solutions in the form: $\psi = \rho\, e^{i\Theta}$;

  the *total* electric potential is then: $\phi \approx \epsilon\, \rho\, \cos(\mathbf{kr} - \omega t + \Theta)$

  where the *amplitude* ρ and *phase correction* Θ depend on ζ, τ.

- Bright–type envelope soliton (pulse):

$$\rho = \rho_0\, \mathrm{sech}\left(\frac{\zeta - v\,\tau}{L}\right), \qquad \Theta = \frac{1}{2P}\left[v\,\zeta - (\Omega + \frac{1}{2}v^2)\tau\right].$$

$$L = \sqrt{\frac{2P}{Q}}\frac{1}{\rho_0}$$

This is a propagating (and *oscillating*) localized pulse:

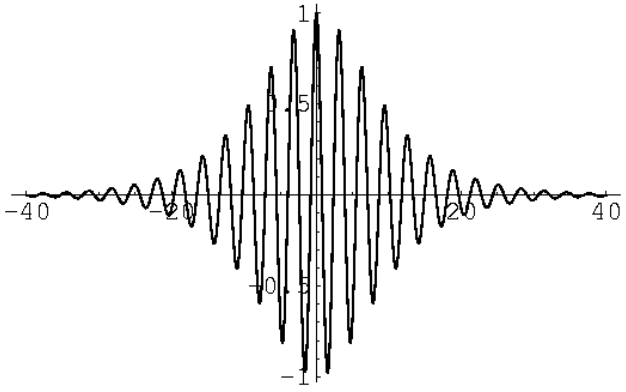

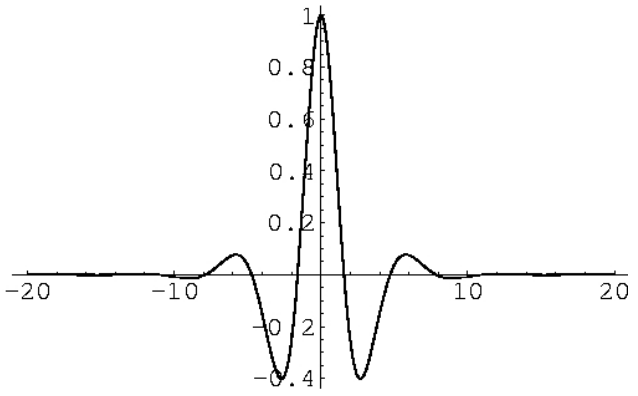

Propagation of a bright envelope soliton (pulse)

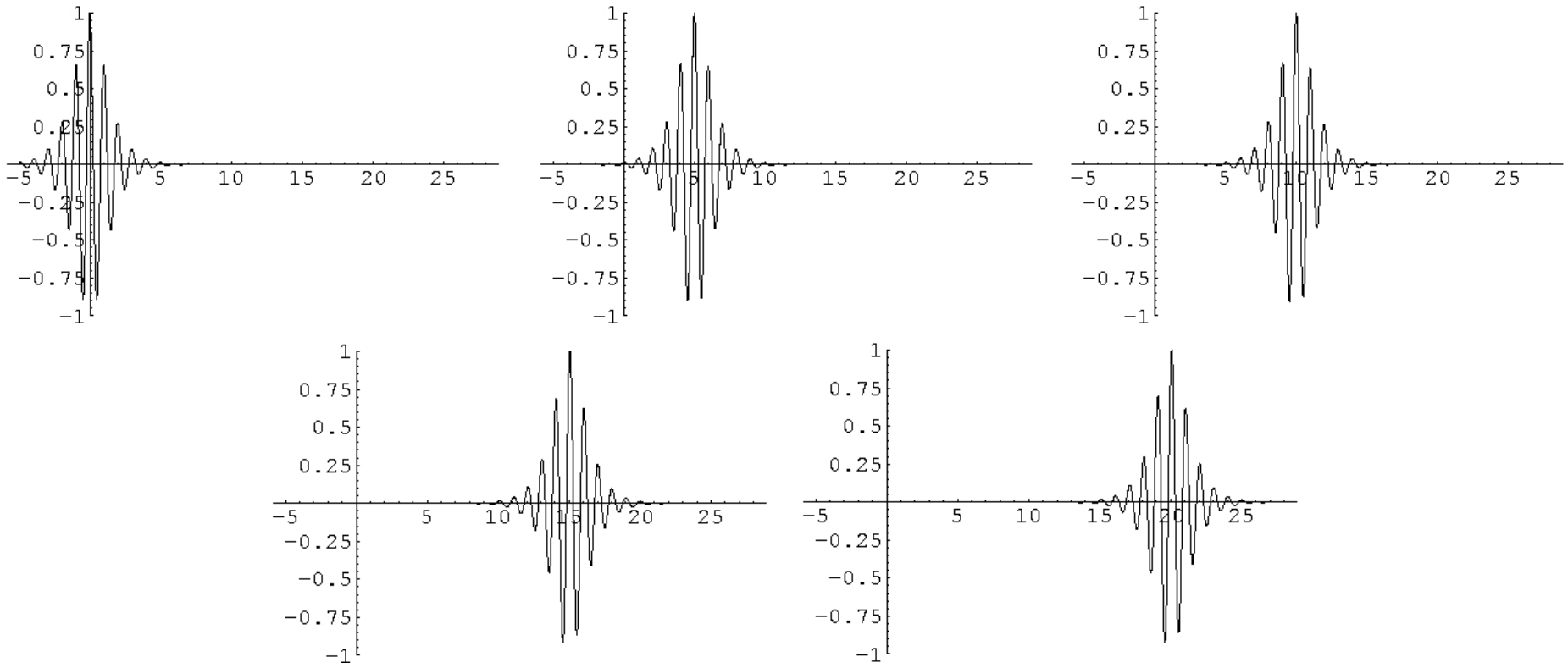

Propagation of a bright envelope soliton (pulse)

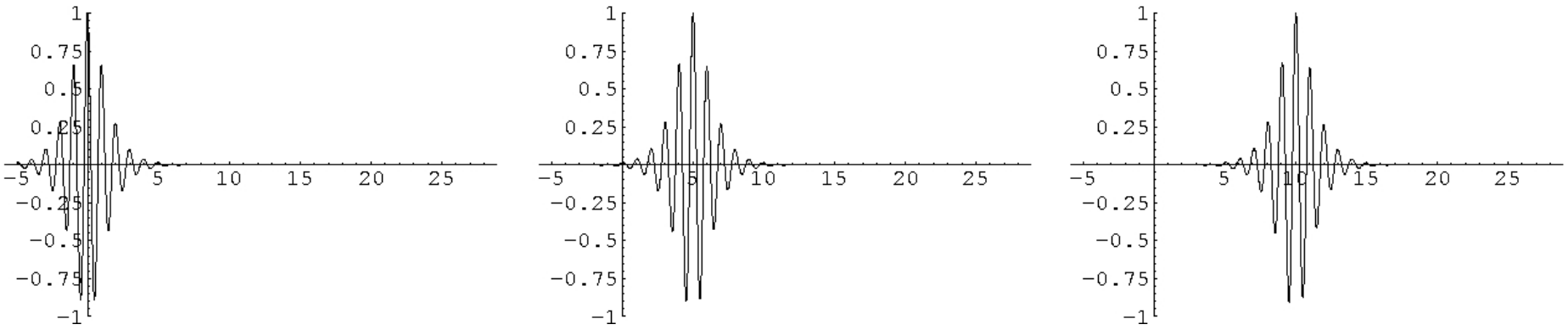

Cf. electrostatic plasma wave data from satellite observations:

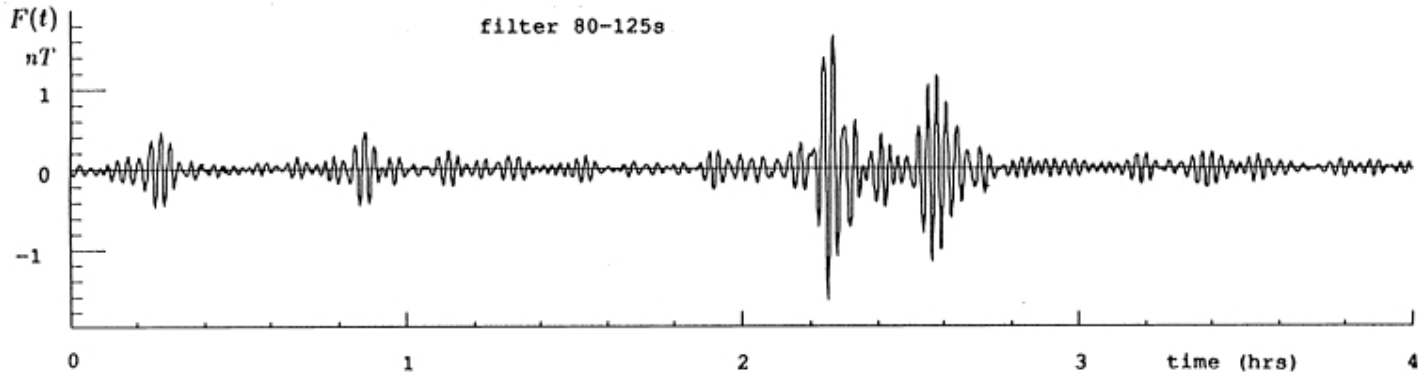

(from: [Ya. Alpert, Phys. Reports **339**, 323 (2001)])

Propagation of a bright envelope soliton (continued...)

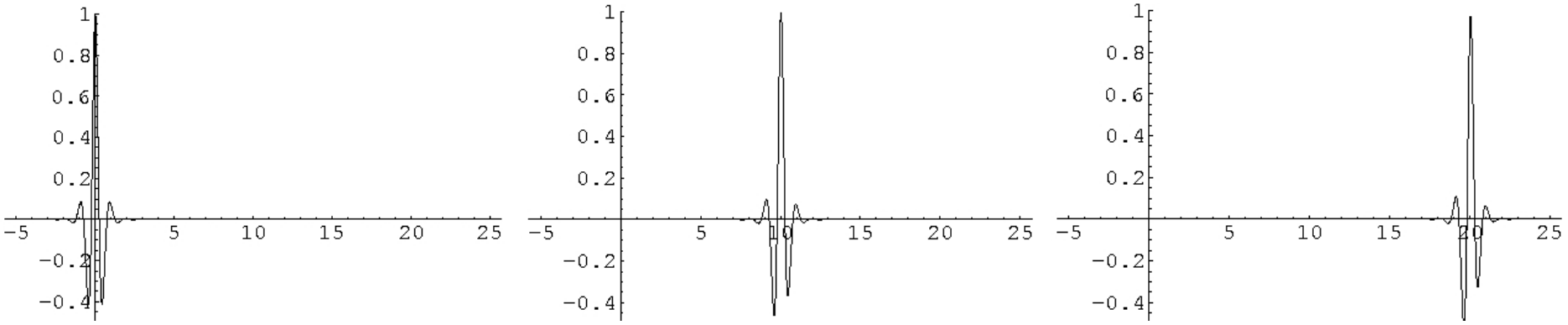

Propagation of a bright envelope soliton (continued...)

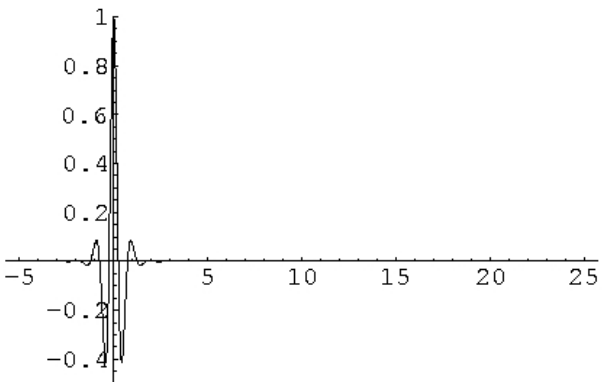

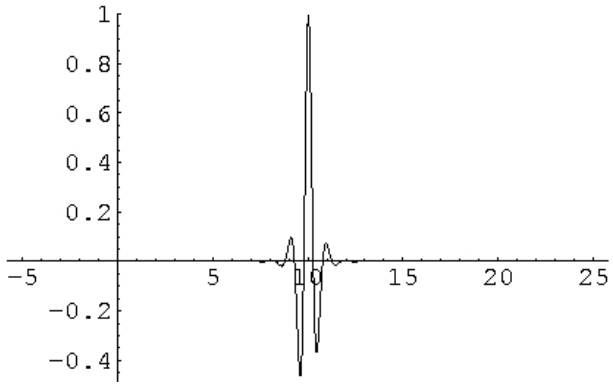

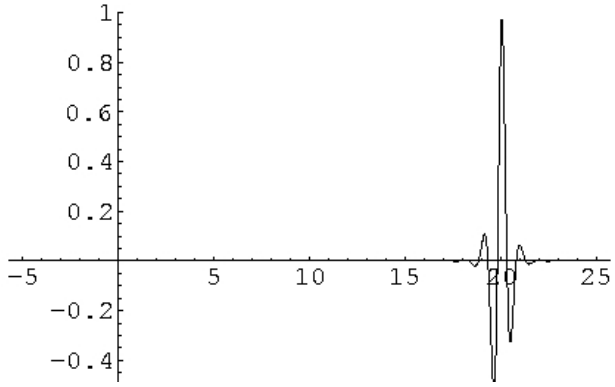

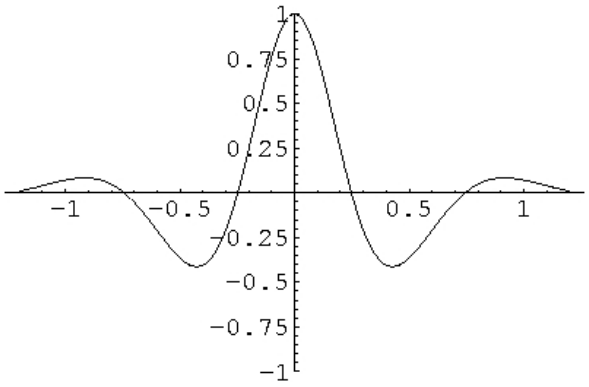

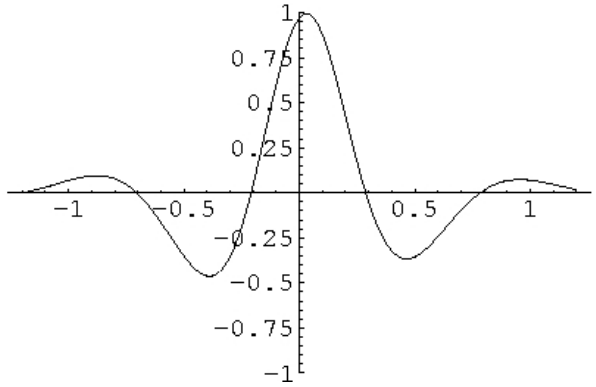

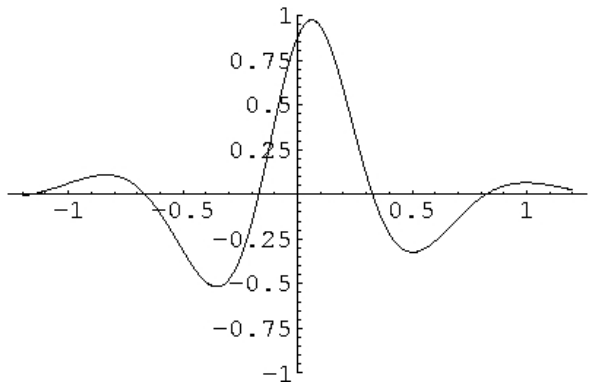

Propagation of a bright envelope soliton (continued...)

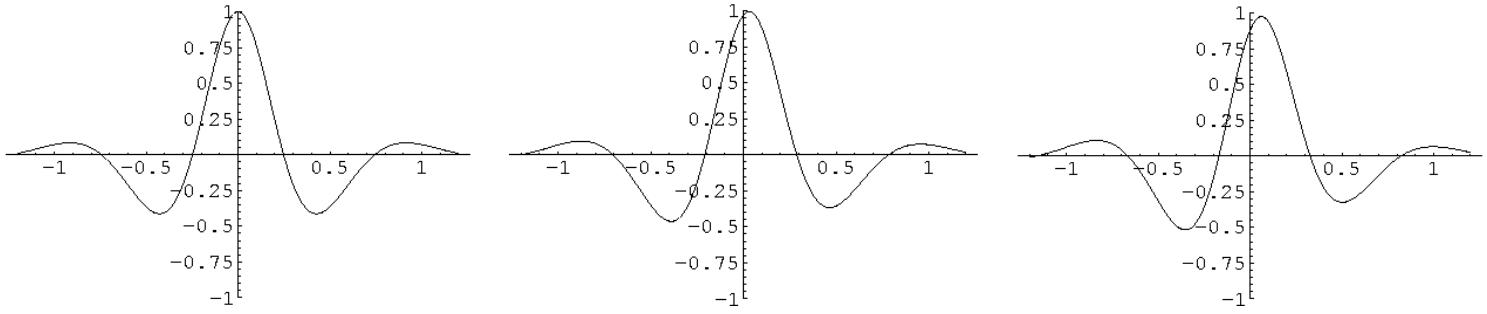

Rem.: *Time-dependent phase* $\rightarrow$ *breathing* effect (at rest frame):

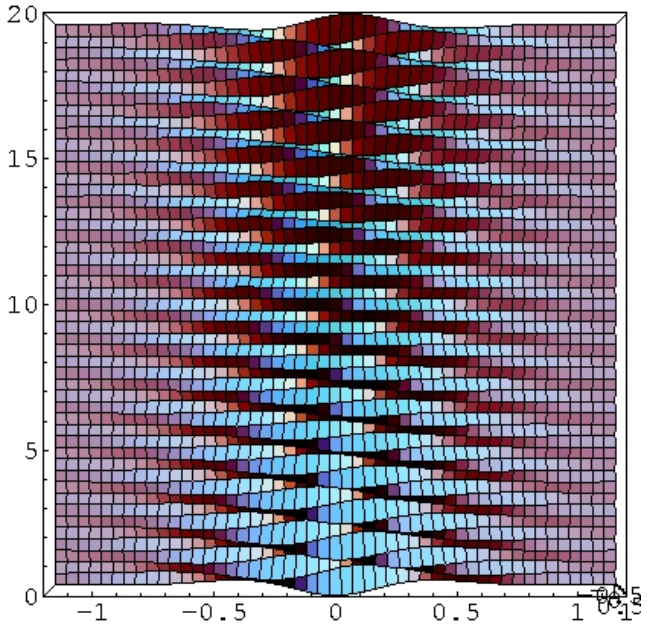

Localized envelope excitations

- Dark–type envelope solution (*hole soliton*):

$$\rho = \pm\rho_1\left[1-\mathrm{sech}^2\left(\frac{\zeta-v\tau}{L'}\right)\right]^{1/2} = \pm\rho_1\tanh\left(\frac{\zeta-v\,\tau}{L'}\right),$$

$$\Theta = \frac{1}{2P}\left[v\,\zeta-\left(\frac{1}{2}v^2-2PQ\rho_1^2\right)\tau\right]$$

$$L' = \sqrt{2\left|\frac{P}{Q}\right|}\frac{1}{\rho_1}$$

This is a *propagating localized hole* (zero density void):

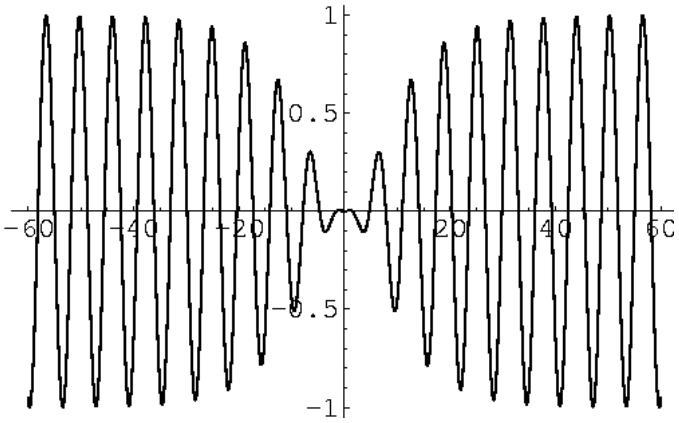

Localized envelope excitations

- Grey–type envelope solution (*void soliton*):

$$\rho = \pm\rho_2 \left[1 - a^2 \,\mathrm{sech}^2\left(\frac{\zeta - v\,\tau}{L''}\right)\right]^{1/2}$$

$$\Theta = \ldots$$

$$L'' = \sqrt{2\left|\frac{P}{Q}\right|}\frac{1}{a\rho_2}$$

This is a propagating *(non zero-density)* void:

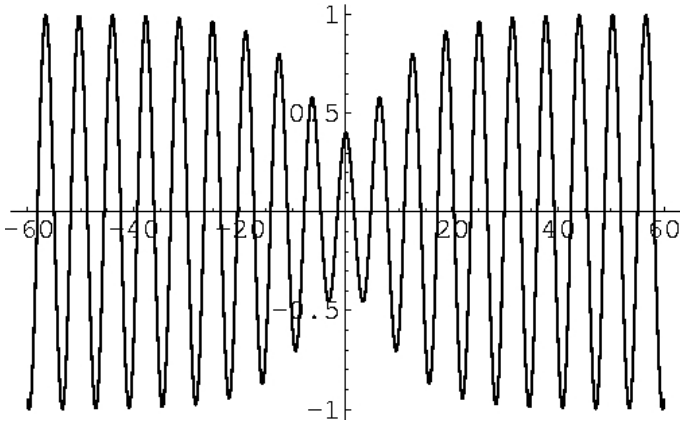

Envelope solitons in action (1): *anomalous* vs. *normal* dispersion

Case $PQ > 0$ (**"Anomalous dispersion"**): stable bright (left plot)/ unstable dark (right plot) envelopes:

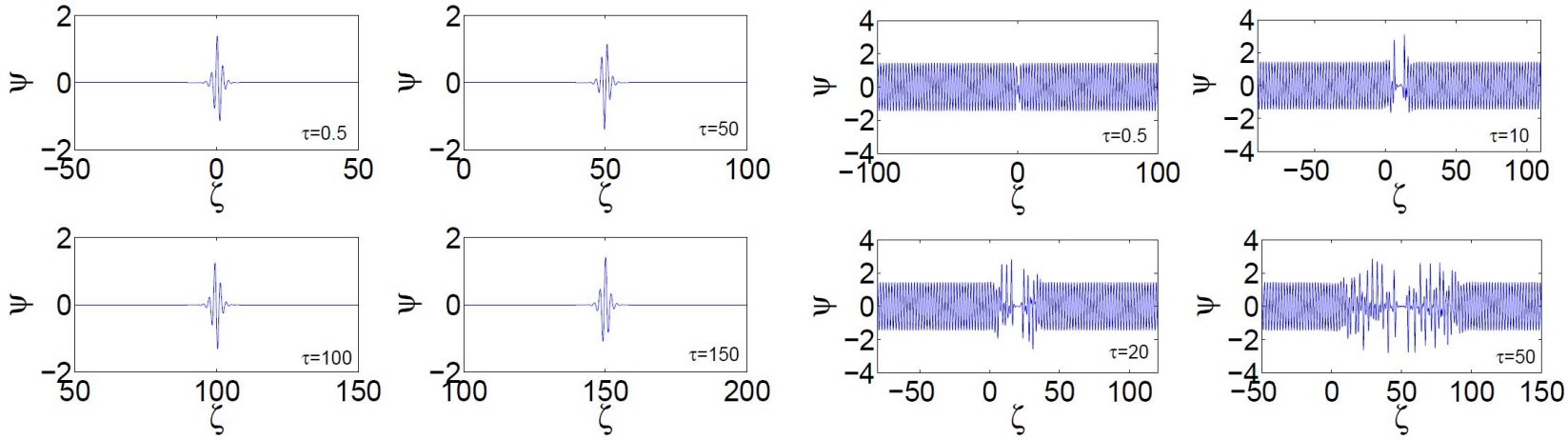

Case $PQ < 0$ (**"Normal dispersion"**): unstable bright (left plot) / stable dark (right plot) envelopes:

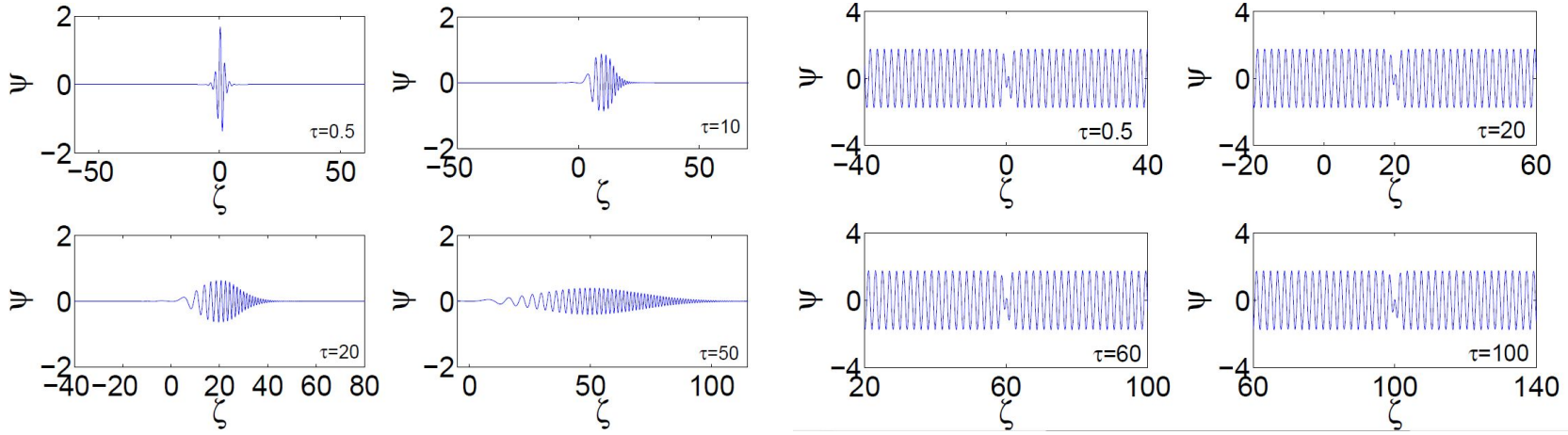

[Numerical results by Sharmin Sultana, Queen's University Belfast.]

Envelope solitons in action (2): *anomalous* vs. *normal* dispersion

Bright envelope solitons on the space-time plane: stable vs unstable:

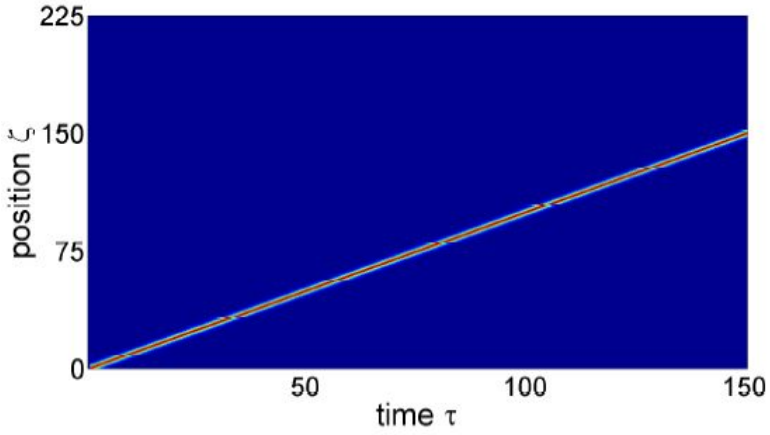

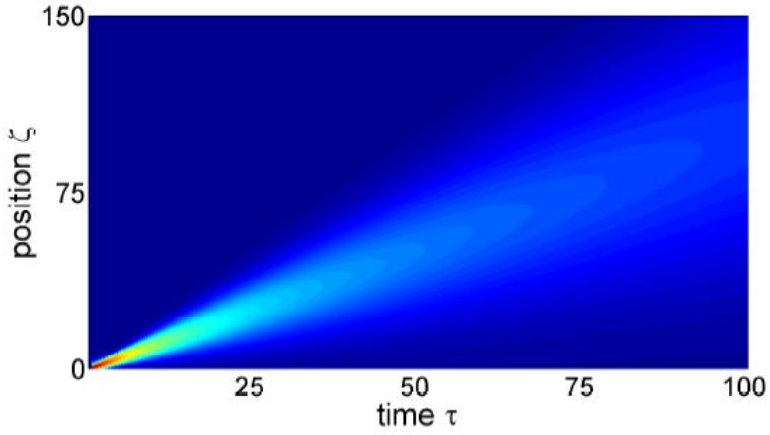

Dark-type envelope solitons on the space-time plane: stable vs unstable:

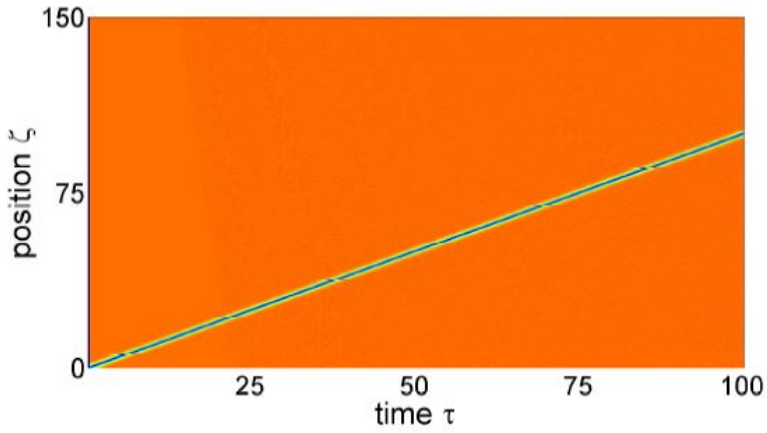

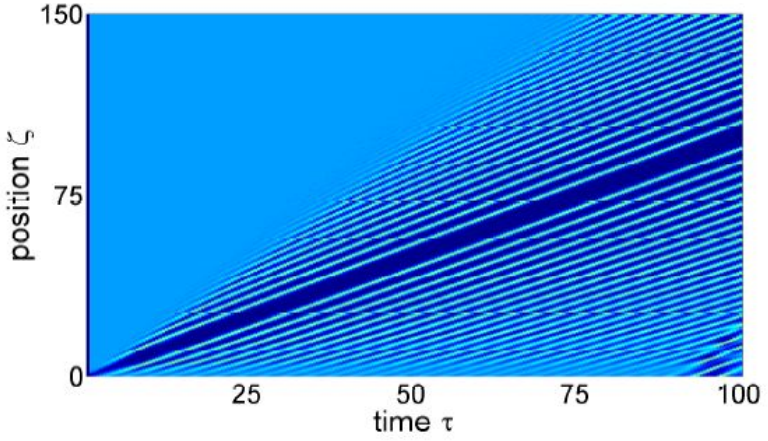

[Numerical results by Sharmin Sultana, Queen's University Belfast.]

Modulational (in)stability: parametric dependence

Both the *instability growth rate* and *threshold* $k_{critical}$ depend on the plasma parameters in a non-trivial (and non-monotonic) manner:

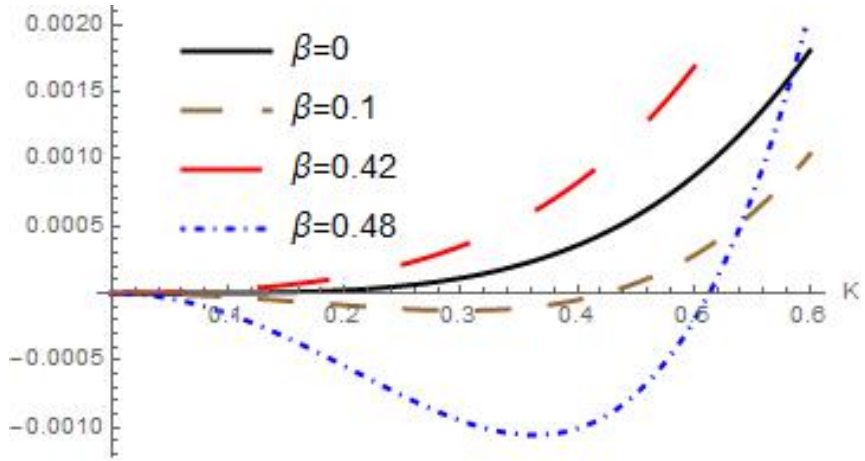

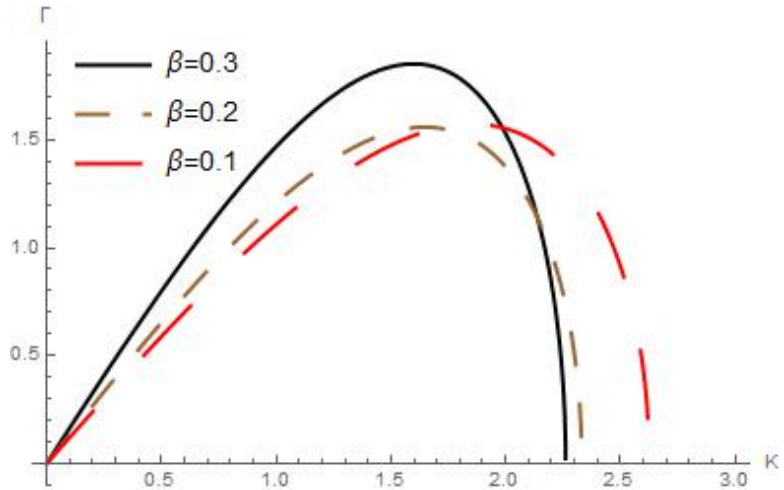

Nonlinearity coefficient: parametric dependence

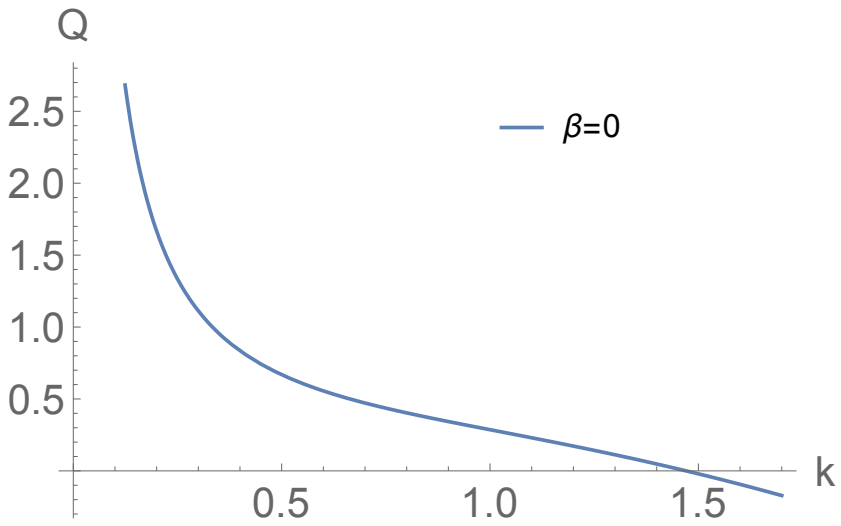

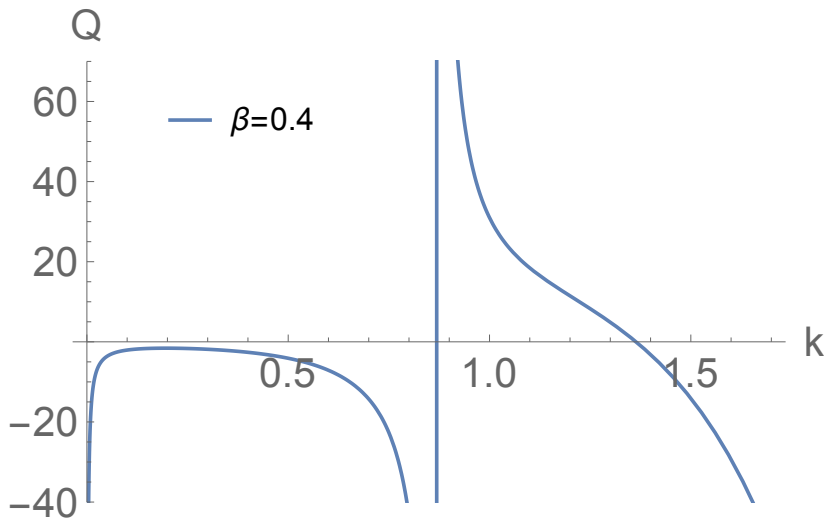

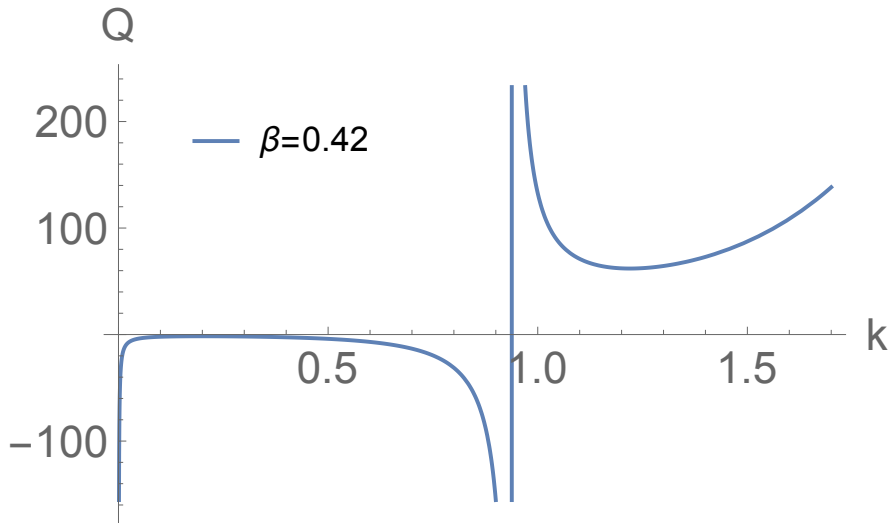

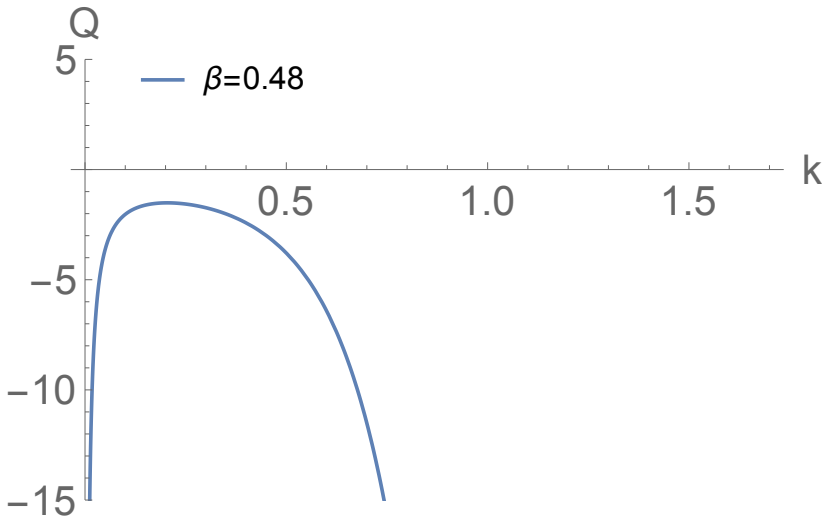

Nonlinearity coefficient: parametric dependence

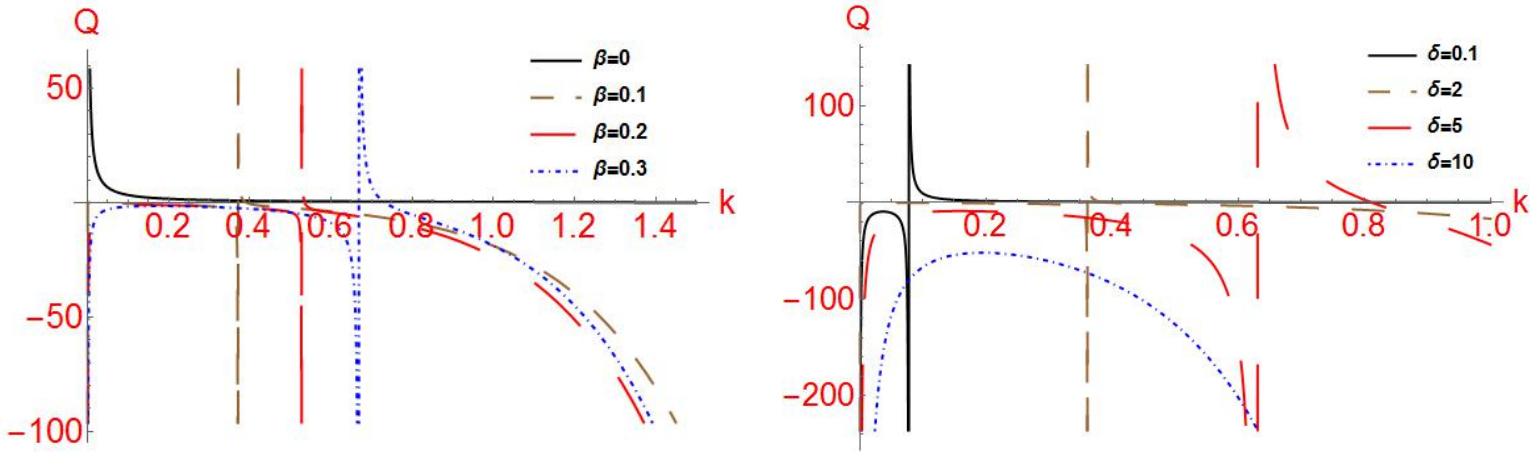

- In the long-wavelength limit $k \ll 1$: $P \simeq p_0\, k$ and $Q \simeq q_0\, k^{-1}$, where:

$$p_0 = -\frac{3\sqrt{1+\delta\beta}}{2(1-\beta)^{3/2}}\,, \qquad q_0 = -\frac{\sqrt{1-\beta}\left[2+2\delta^2\beta^2-\beta(3+2\delta+3\delta^2)\right]^2}{12+(1+\delta\beta)^{7/2}}\,.$$

- Recall that the ratio P/Q determines the geometry of envelope solitons ($L \sim (P/Q)^{1/2}$), as well as the criterion for their existence.

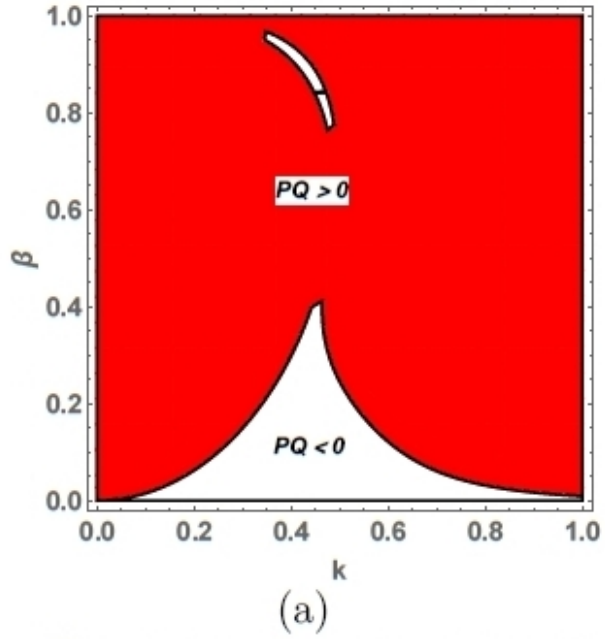

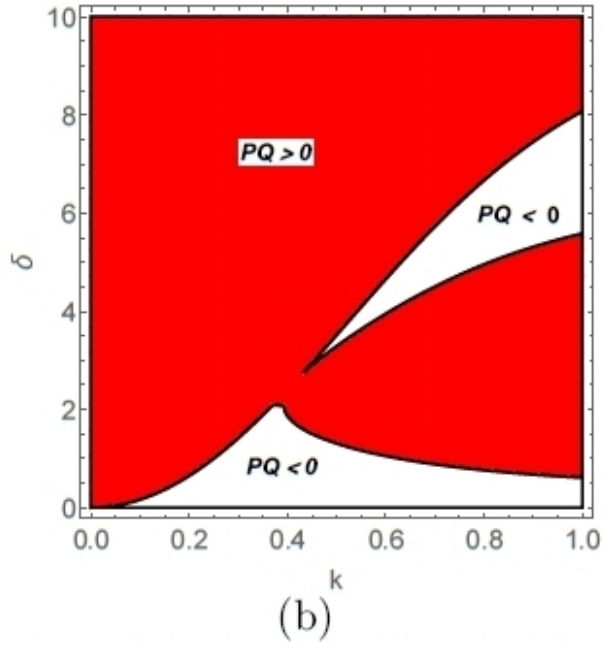

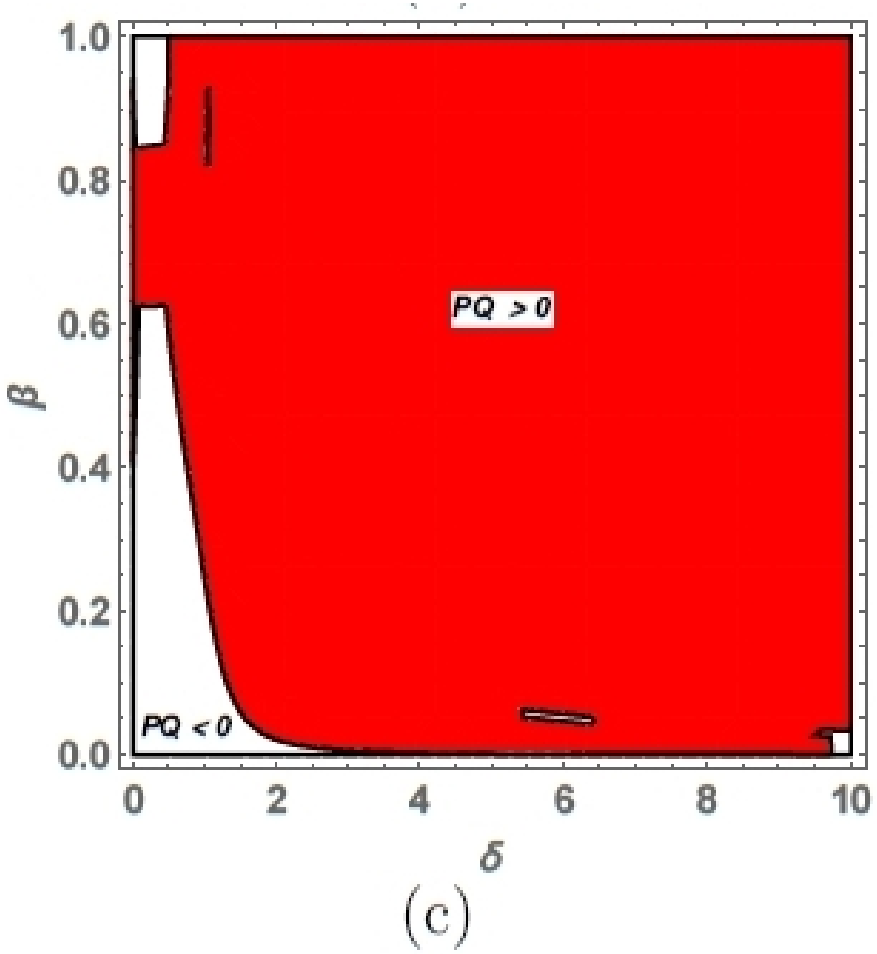

FIG. 9: (Color online) Region for $PQ < 0$ (white region) and $PQ > 0$ (red region) as functions of the wave number k and(a) β when $\delta = 1$, (b) δ when $\beta = 0.1$. (c) β and δ when $k = 0.5$.

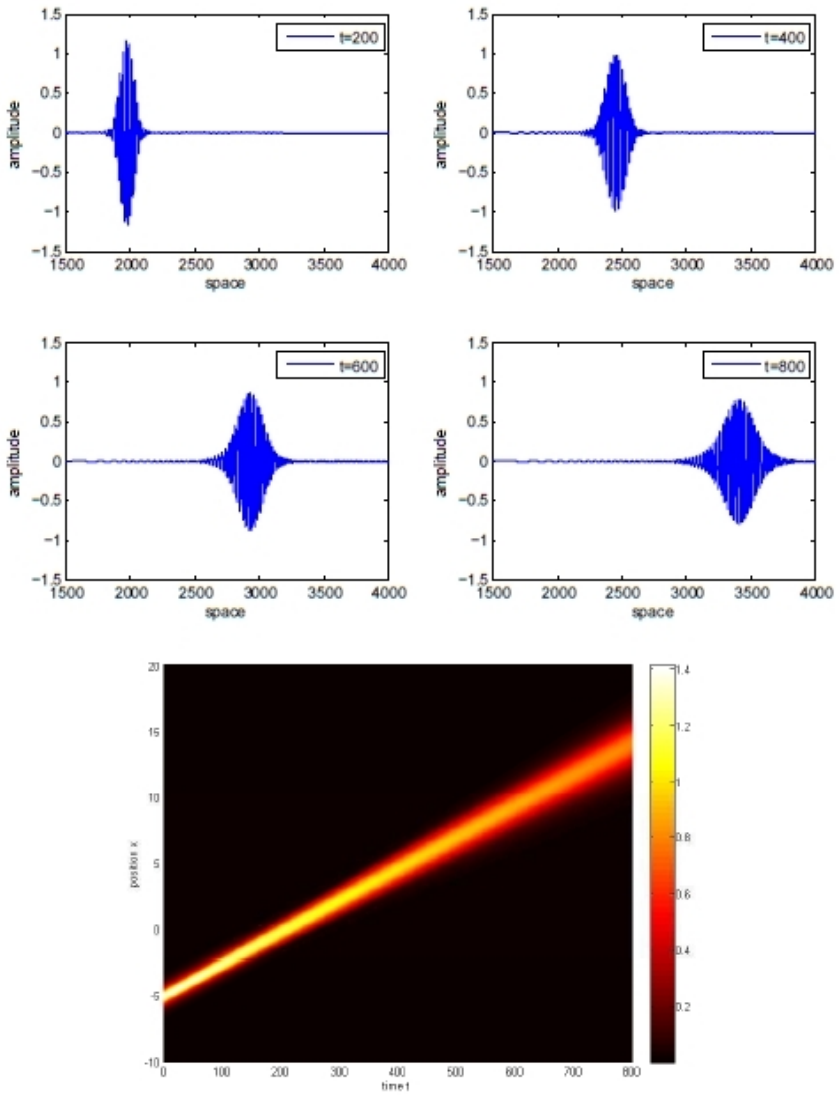

FIG. 18: (Color online) Time evolution and propagation of a breather (bright soliton) on the space-time plane. IC ($\beta = 0.1, \delta = 1, k = 0.1,\ PQ > 0$), NLSE ($\beta = 0.2, \delta = 1, k = 0.1,\ PQ > 0$).

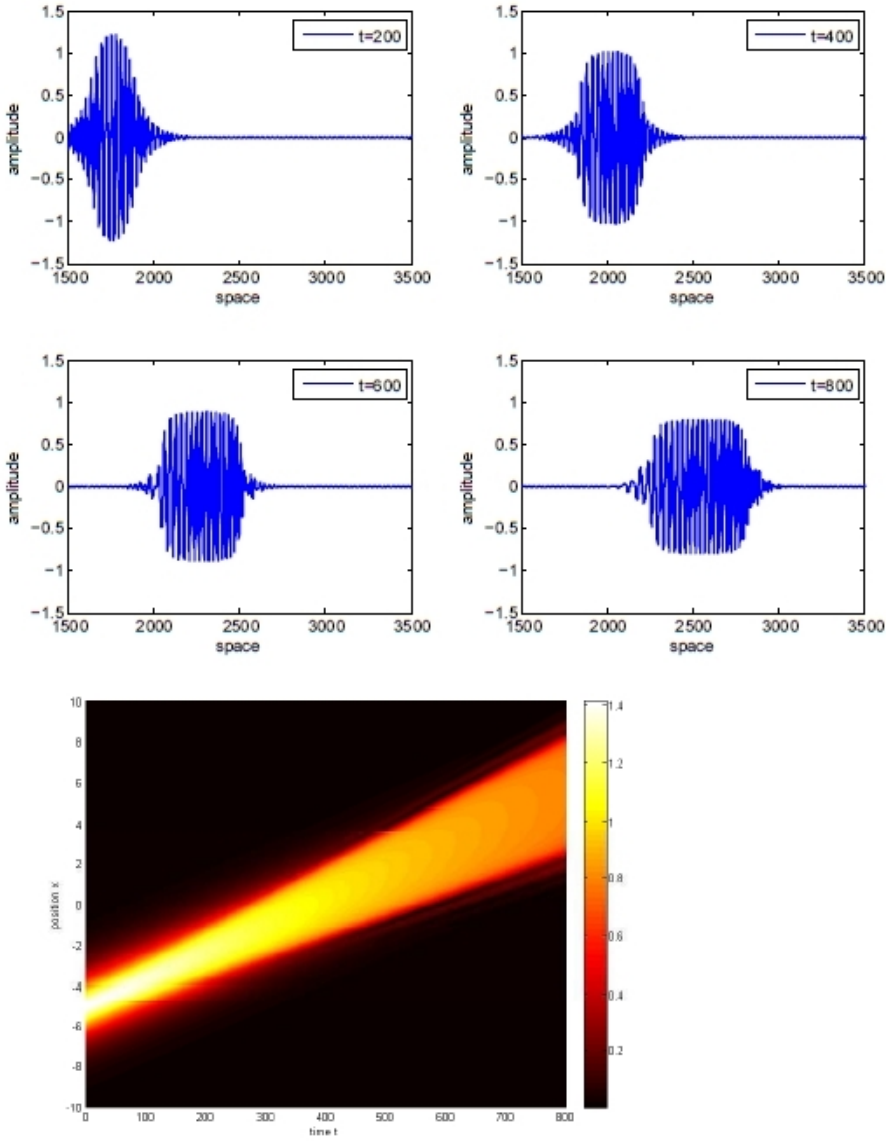

FIG. 19: (Color online) Time evolution and propagation of a breather (bright soliton) on the space-time plane. IC ($\beta = 0.2, \delta = 1, k = 0.1,\ PQ > 0$), NLSE ($\beta = 0, \delta = 1, k = 0.1,\ PQ < 0$).

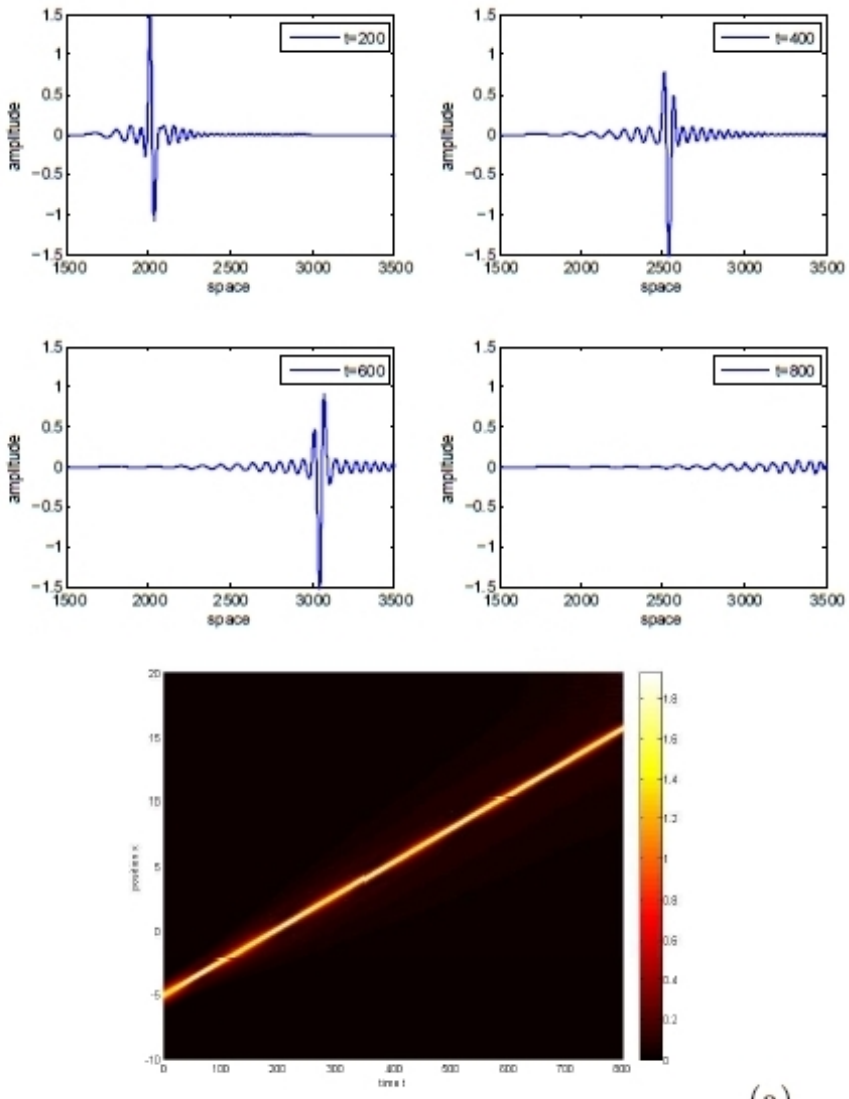

(a)

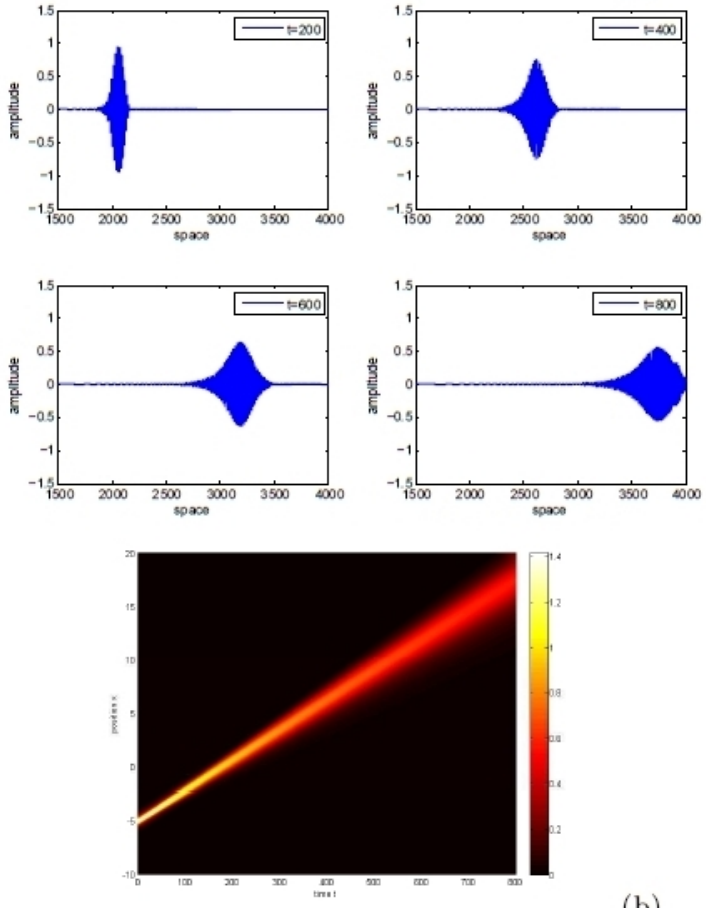

(b)

FIG. 20: (Color online) Time evolution and propagation of a breather (bright soliton) on the space-time plane. (a) IC ($\beta = 0.2, \delta = 1, k = 0.1,\ PQ > 0$), NLSE ($\beta = 0.4, \delta = 2.1, k = 0.7,\ PQ > 0$).(b) IC ($\beta = 0, \delta = 1, k = 0.1,\ PQ < 0$), NLSE ($\beta = 0.2, \delta = 1, k = 0.1,\ PQ > 0$).

Critical carrier wavenumber (threshold) versus negative ion concentration (β)

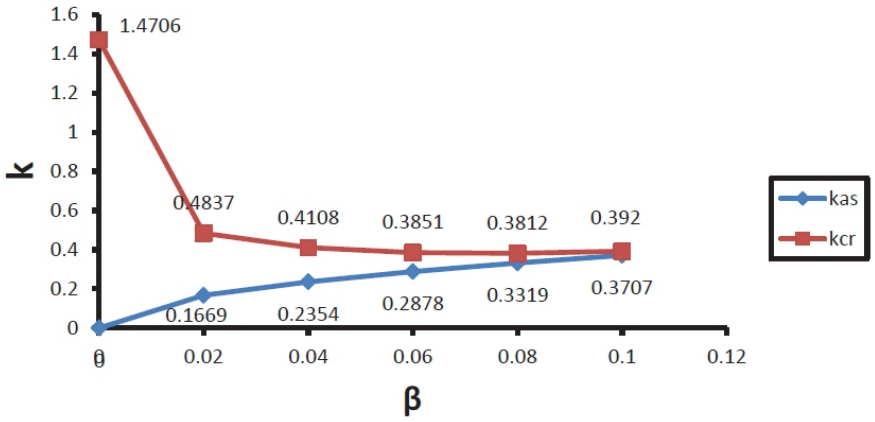

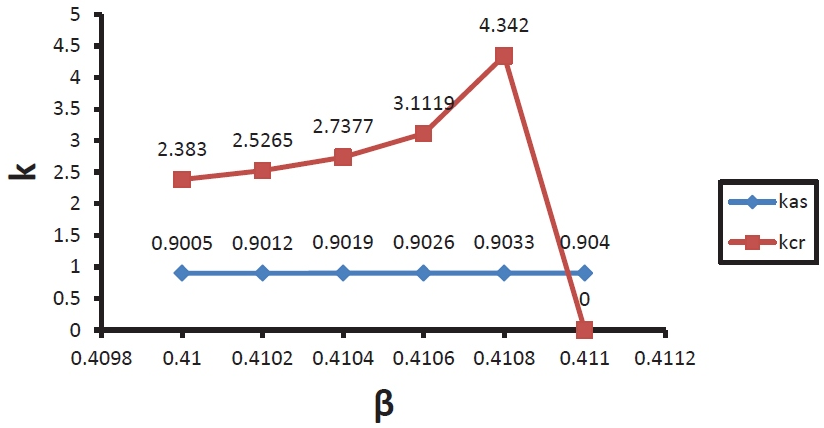

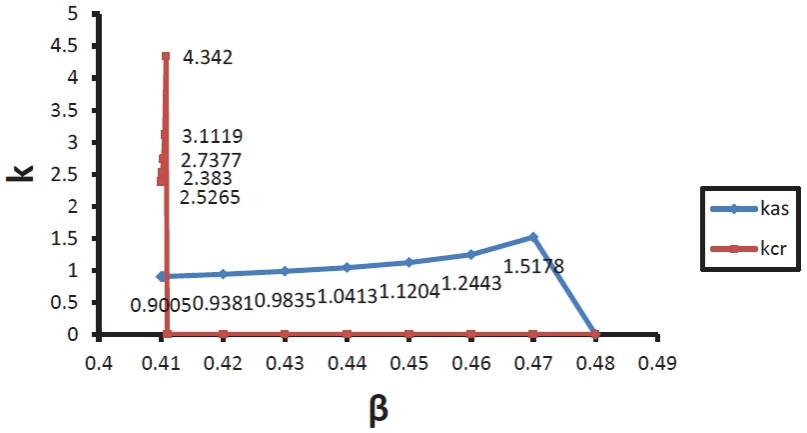

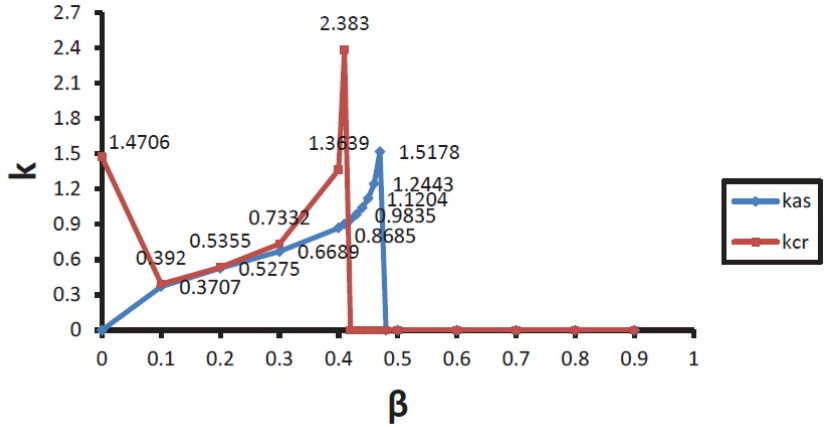

Part 4: Analytical models for rogue waves

Various solutions of the NLS equation have been proposed as model candidates for rogue waves:

- The *Peregrine soliton*

  [D. H. Peregrine, J. Austral. Math. Soc. B **25**, 16 (1983); K. B. Dysthe, and K. Trulsen, Physica Scripta **T82**, 48 (1999); V. I. Shrira, and V. V. Geogjaev, J. Eng. Math. **67**, 11 (2010); B. Kibler, J. Fatome, et al., Nature Physics **6**, 790 (2010)]

- The *Kuznetsov-Ma breather*

  [Ya C. Ma, Stud. Appl. Math. **60**, 43 (1979)];

- The *Akhmediev breather*

  [N. N. Akhmediev, V. M. Eleonskii, and N. E. Kulagin, Theor. Math. Phys. 72, 809 (1987)];

- Higher-order rational solutions of the NLSE.

In the following, we have considered the above paradigms, with an aim to investigate their dependence on relevant plasma parameters.

Peregrine Soliton as a model for rogue waves

- As a first approach to rogue waves, we consider the Peregrine soliton:

$$\psi(\xi,\tau)=\left[1-\frac{4(1+i2Q\tau)}{1+2Q\xi^2/P+4Q^2\tau^2}\right]\exp\left(iQ\tau\right)$$

[D. H. Peregrine, J. Austral. Math. Soc. B **25**, 16 (1983); K. B. Dysthe & K. Trulsen, Physica Scripta **T82**, 48 (1999); V. I. Shrira & V. V. Geogjaev, J. Eng. Math. **67**, 11 (2010); B. Kibler, *et al.*, Nat. Phys. **6**, 790 (2010)]

- The Peregrine paradigm as a prototypical model for rogue waves has recently been employed successfully in NL optics [Kibler *et al*, Nat. Phys. (2010)];

- Recalling the functional dependence of P and Q on plasma parameters, this model allows one to investigate the parametric dependence on the plasma configurational parameters and the wavenumber k (reduced variables).

LETTERS
PUBLISHED ONLINE: 22 AUGUST 2010 | DOI: 10.1038/NPHYS1740
nature physics

The Peregrine soliton in nonlinear fibre optics

B. Kibler[1], J. Fatome[1], C. Finot[1], G. Millot[1], F. Dias[2,3], G. Genty[4], N. Akhmediev[5] and J. M. Dudley[6]*

The Peregrine soliton is a localized nonlinear structure predicted to exist over 25 years ago, but not so far experimentally observed in any physical system[1]. It is of fundamental significance because it is localized in both time and space, and because it defines the limit of a wide class of solutions to the nonlinear Schrödinger equation (NLSE). Here, we use an analytic

Our experiments are designed using the breather formalism of ref. 2. With dimensionless field $\psi(\xi,\tau)$, the self-focusing NLSE is:

$$i\frac{\partial\psi}{\partial\xi}+\frac{1}{2}\frac{\partial^2\psi}{\partial\tau^2}+|\psi|^2\psi=0 \qquad (1)$$

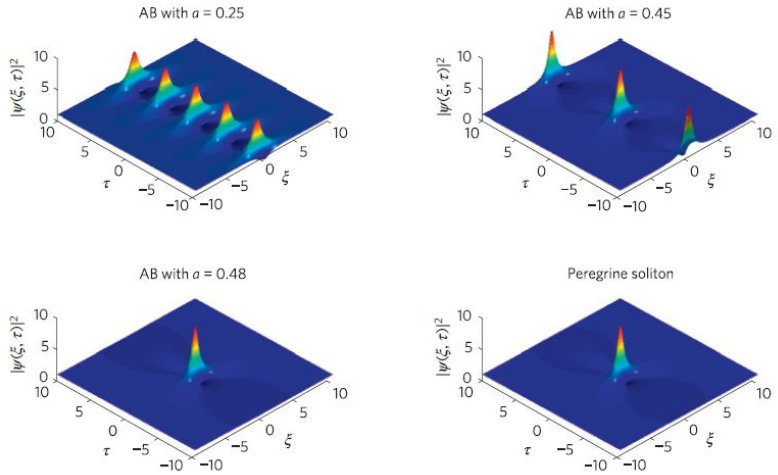

Figure 1 | Plotted Akhmediev breather solutions using equation (2) for modulation parameter $a = 0.25$, $a = 0.45$ and $a = 0.48$, as well as the ideal **Peregrine soliton of equation (3), the limiting case of the Akhmediev breather as $a \to 1/2$.** Maximum temporal compression occurs at normalized distance $\xi = 0$. The differences between the Akhmediev breather (AB) with $a = 0.48$ and the Peregrine soliton can be seen with close inspection of the decay of the peak to the wings; they are shown more clearly in Fig. 2.

[B. Kibler, J. Fatome, C. Finot, G. Millot, F. Dias, G. Genty, N. Akhmediev & JM Dudley, Nat. Phys. **6**, 790 (2010)]

PRL 107, 255005 (2011) PHYSICAL REVIEW LETTERS week ending 16 DECEMBER 2011

Observation of Peregrine Solitons in a Multicomponent Plasma with Negative Ions

H. Bailung,[1] S. K. Sharma,[1] and Y. Nakamura[1,2]

[1]*Plasma Physics Laboratory, Physical Sciences Division, Institute of Advanced Study in Science and Technology, Paschim Boragaon, Guwahati-35, India*

[2]*On leave from Yokohama National University, Yokohama, Japan*

(Received 29 July 2011; published 16 December 2011)

The experimental observation of Peregrine solitons in a multicomponent plasma with the critical concentration of negative ions is reported. A slowly amplitude modulated perturbation undergoes self-modulation and gives rise to a high amplitude localized pulse. The measured amplitude of the Peregrine soliton is 3 times the nearby carrier wave amplitude, which agrees with the theory. The numerical solution of the nonlinear Schrödinger equation is compared with the experimental results.

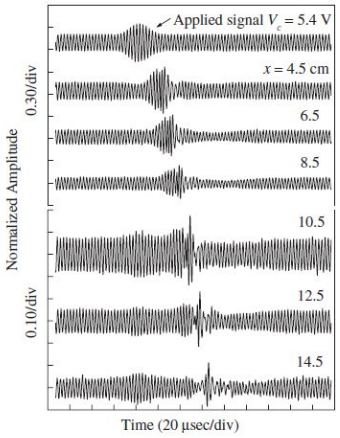

FIG. 2. Observed signals of the electron density perturbation at different probe positions from the separation grid. The top trace is the applied signal with carrier and modulation frequencies 350 and 31 kHz, respectively. Peak to peak amplitude of the applied carrier wave (V_c) is fixed at 5.4 V. Signals observed at 10.5 to 14.5 cm are shown with different amplitude scale (0.10/div) for better resolution.

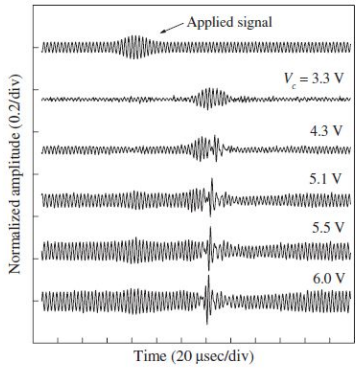

FIG. 3. Signals recorded for different excitation amplitudes of the carrier wave. The probe is fixed at 13.6 cm from the separation grid. Top trace represents the applied signal with carrier and modulation frequencies 350 and 31 kHz, respectively.

[9]. The slight shift in the phase of the carrier part with theory is probably due to the presence of pseudowave in front of the solitons [15]. However, detailed investigation is necessary for confirmation. We analyzed the wave signals

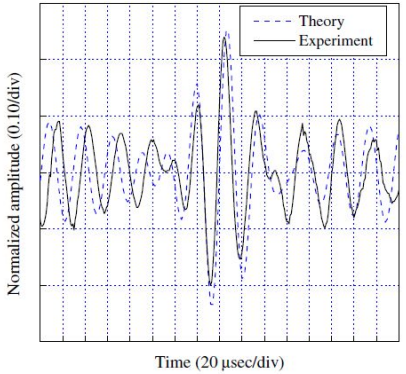

FIG. 4 (color online). Comparison of the time series signal (solid line) observed at 13.6 cm with the theoretical Peregrine soliton (dashed line) obtained by using Eq. (3). The applied carrier and modulation frequencies are 350 and 31 kHz, respectively. $V_c = 5.9$ V. The parameters used for numerical calculations are $\omega = 0.7\omega_{pi}$, ($\omega_{pi} = 492$ kHz), $k = 0.74k_D$, $k_D = 1/\lambda_D = 20.0$ cm^{-1}.

[H. Bailung, S.K. Sharma and Y. Nakamura, PRL 107, 255005 (2011)]

Kuznetsov-Ma breather as a model for rogue waves

- *Kuznetsov - Ma breather*:

$$\psi(\xi,\tau) = \left[\frac{\cos(\frac{1}{2}s'Q\tau - 2i\phi) - \cosh\phi\cosh\left(s\sqrt{\frac{Q}{2P}}\xi\right)}{\cos(\frac{1}{2}s'Q\tau) - \cosh\phi\cosh\left(s\sqrt{\frac{Q}{2P}}\xi\right)}\right]\exp\left(iQ\tau\right)$$

where $\phi \in \Re\,, \qquad s = 2\sinh\phi\,, \qquad s' = 2\sinh(2\phi)$

[Credit: Ya C. Ma, *Stud. Appl. Math.* **60**, 43 (1979).]

- The KM breather was observed in optical fibers [Kibler *et al*, Nature/Sci. Rep. (2012)];

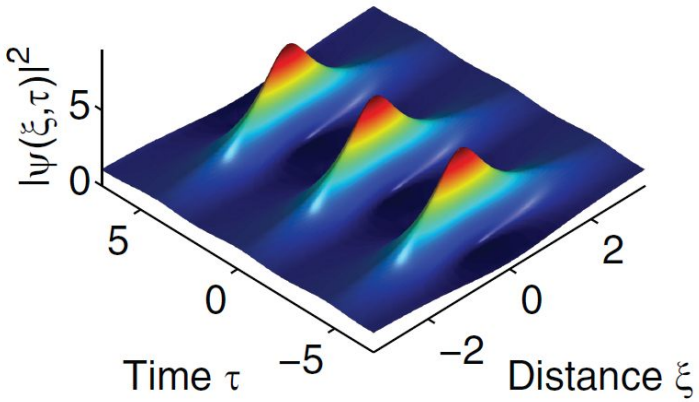

Akhmediev breather as a model for rogue waves

$$\psi(\xi,\tau) = \left[1 + \frac{2(1-2a)\cosh(bQ\tau) + ib\sinh(bQ\tau)}{\sqrt{2a}\cos\left(\omega\sqrt{\frac{Q}{2P}}\xi\right) - \cosh(bQ\tau)}\right]\exp\left(iQ\tau\right)$$

where

$$\alpha \in (0, 1/2]\,, \qquad \omega = 2\sqrt{1-2\alpha}\,, \qquad b = \sqrt{8a(1-2a)}\ .$$

[Credit: N. Akhmediev, V. M. Eleonskii and N. E. Kulagin, Theor. Math. Phys. **72**, 809 (1987).]

- The A-breather is periodic in space, but localized in time:

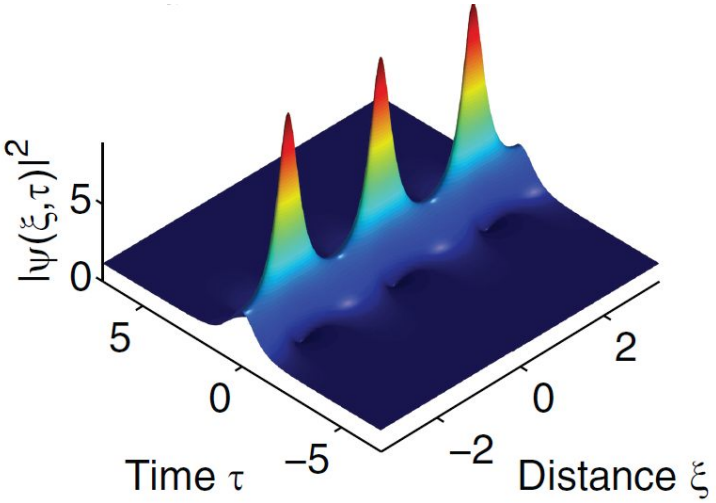

[Figure from: Kibler *et al*, Nat. Phys. (2010) & Nature/Sci.Rep. (2012).]

Akhmediev breather as a model for rogue waves

$$\psi(\xi,\tau)=\left[1+\frac{2(1-2a)\cosh(bQ\tau)+ib\sinh(bQ\tau)}{\sqrt{2a}\cos\left(\omega\sqrt{\frac{Q}{2P}}\xi\right)-\cosh(bQ\tau)}\right]\exp\left(iQ\tau\right)$$

where

$$\alpha\in(0,1/2]\,,\qquad \omega=2\sqrt{1-2\alpha}\,,\qquad b=\sqrt{8a(1-2a)}\ .$$

- The *Peregrine* soliton is recovered in some (aperiodic) limit:

$$\psi_P=\lim_{a\to\frac{1}{2}}\psi_A=e^{iq\tau}\left[1-\frac{4(1+2iq\tau)}{1+\frac{2q}{p}\xi^2+4q^2\tau^2}\right]$$

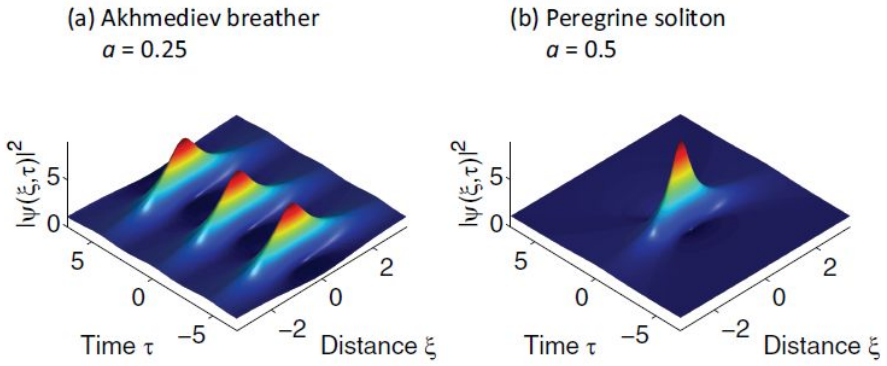

[Credit: Kibler *et al*, Nat. Phys. (2010) & Nature/Sci.Rep. (2012).]

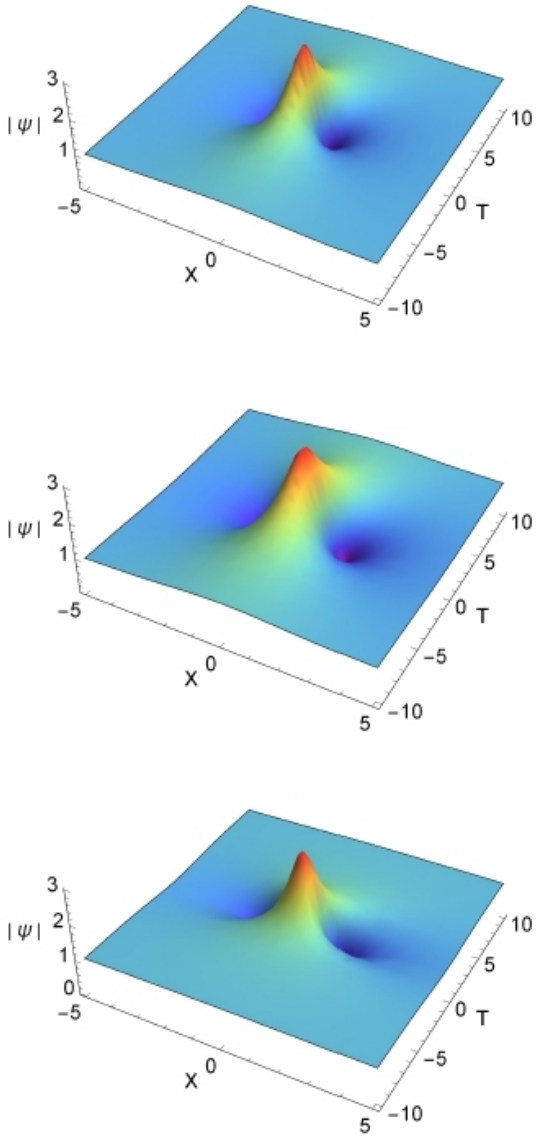

FIG. 15: (Color online) The *Peregrine soliton* is depicted for different values of β $(= 0.2, 0.4, 0.6)$, with $k = 0.1$ and $\delta = 1$ (e.g. for H^+/H^- plasma).

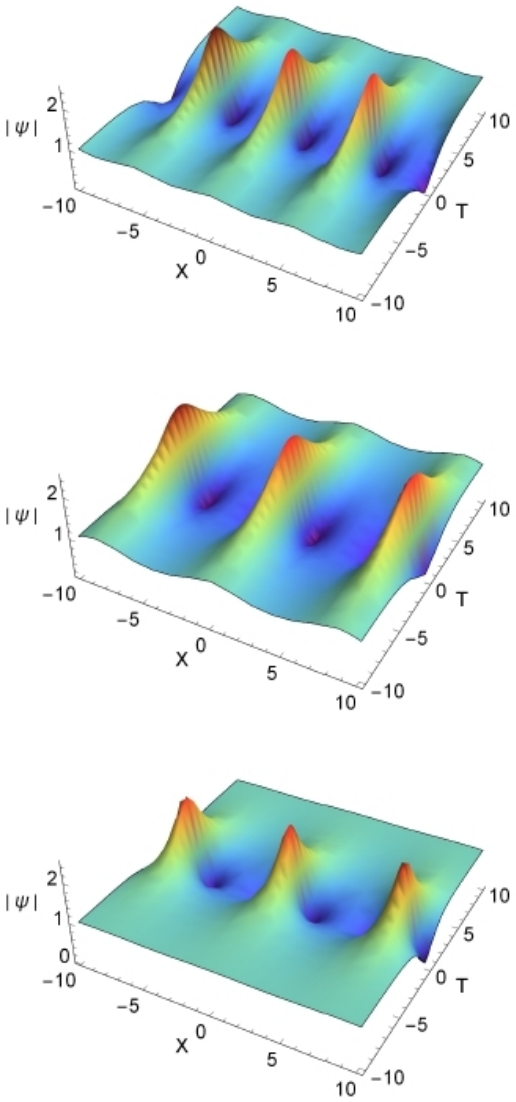

FIG. 16: (Color online) The *Akhmediev breather* is depicted for different values of β $(= 0.2, 0.4, 0.6)$, with $k = 0.1$ and $\delta = 1$ (e.g. for H^+/H^- plasma).

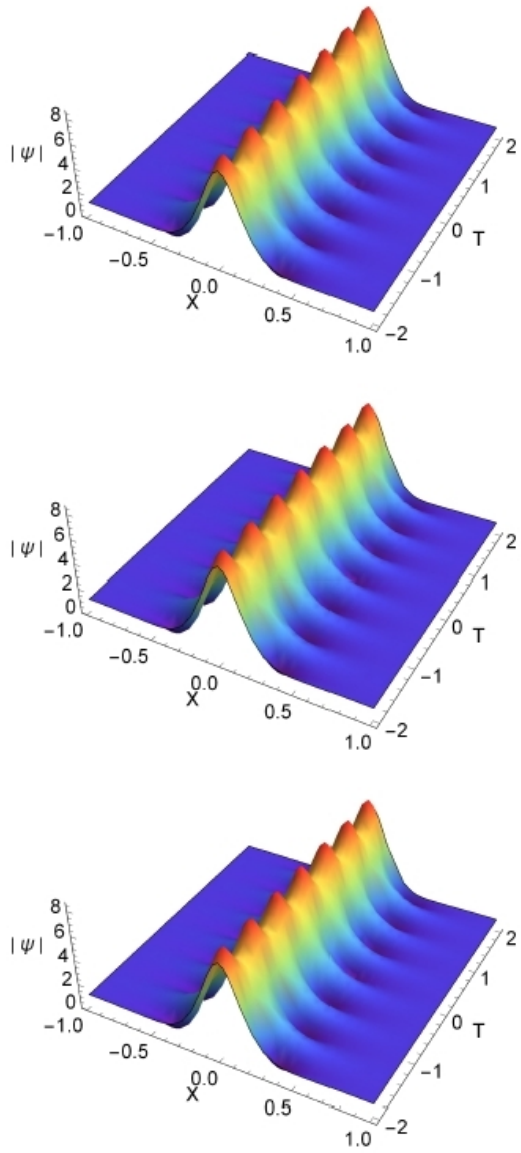

FIG. 17: (Color online) The *Kuznetsov–Ma breather* is depicted for different values of β $(= 0.2, 0.4, 0.6)$, with $k = 0.1$ and $\delta = 1$ (e.g. for H^+/H^- plasma).

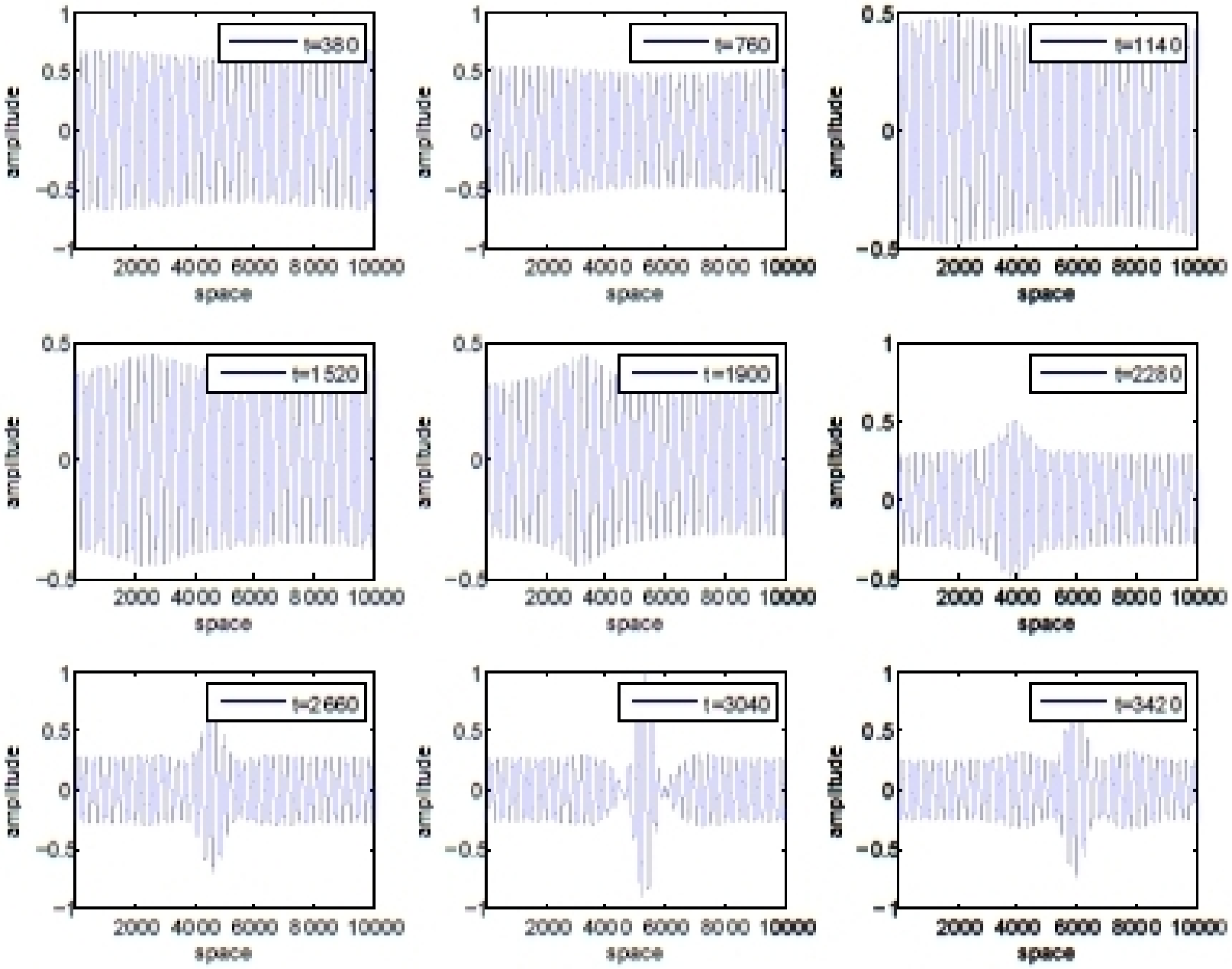
t=380
t=760
t=1140
t=1520
t=1900
t=2280
t=2660
t=3040
t=3420
amplitude
space
2000 4000 6000 8000 10000

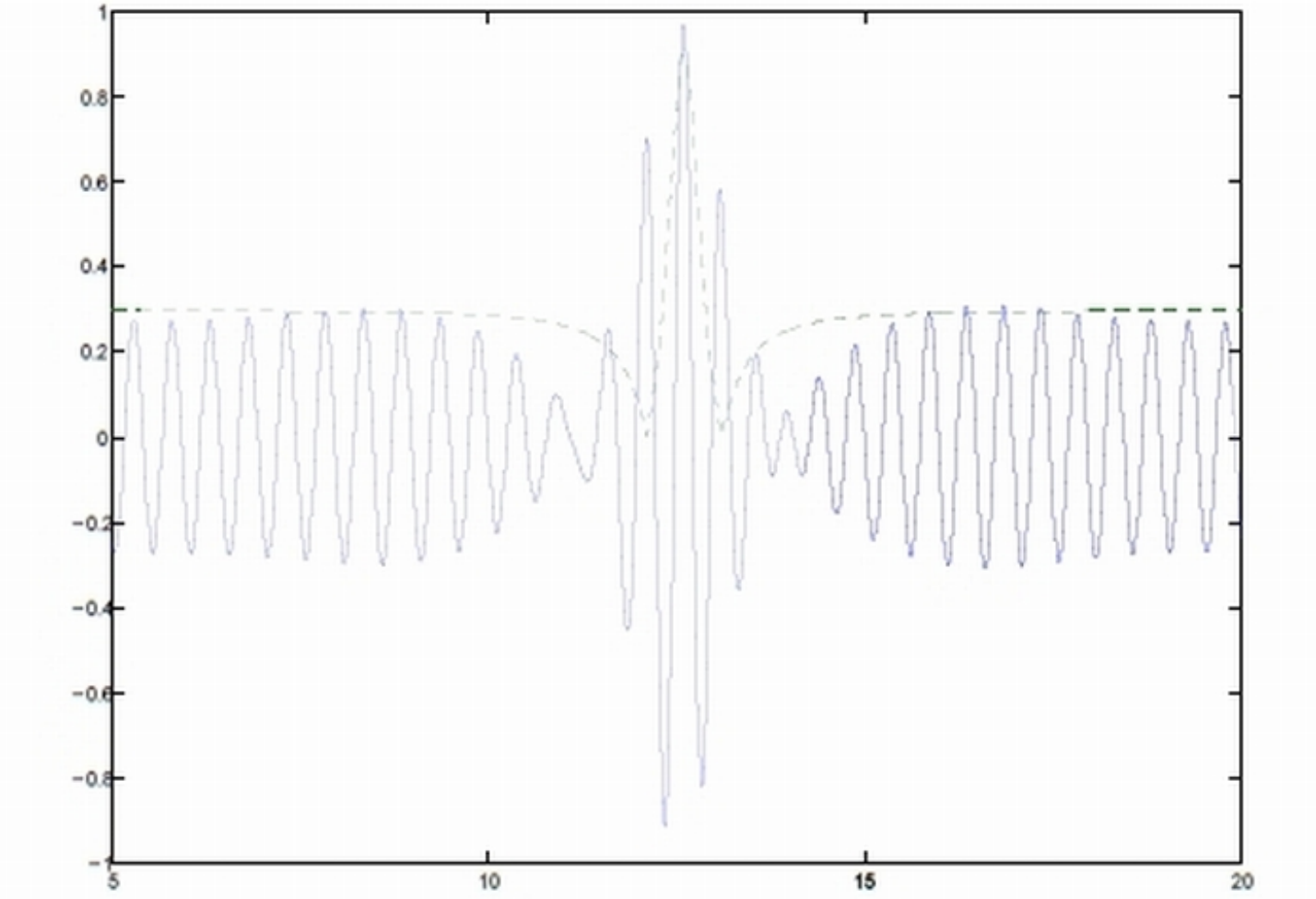

FIG. 21: (Color online) (a)Temporal profiles of the carrier and the growing rogue wave for $PQ > 0$. (b)The envelopes described by the corresponding analytic Peregrine solution of the NLS equation are shown by the dashed (green) curves.

Conclusions & Summary

- Multiscale methodology for ES relativistic solitons revisited
- Powerful analytical technique, provides predictions for

  – Modulational Instability thresholds and growth rate

  – Envelope modes, harmonic generation, rogue waves: possible beyond critical configuration, ***in a wide range of plasma configuration parameters***;
- *Rogue waves* are random events, may be tedious to detect experimentally;
- Results to be compared with experimental results
- Static predictions so far; need for dynamical (numerical) investigation.
- *Work in progress:* fluid simulations, PIC simulations, higher-order breathers, ...

Thanks - credit - acknowledgments

- Ibrahem El-Kamash, Michael McKerr
- ***Vikrant Saxena***, Queen's U. Belfast, UK (currently at DESY, Hamburg, Germany)
- ***Georgios Veldes*** *&* ***Dimitri Franzeskakis***, Uni. Athens, Greece
- ***Evangelos Siminos***, Max-Planck Institut, Dresden, Germany
- ***Gonzalo Sanchez-Ariaga***, Universidad Politecnica Madrid, Spain
- ***Mark Dieckmann*** , Linkoping University, Sweden
- ***Jafar Borhanian***, Uni. Ardabil, Iran

– ***Inspiration & discussions:***

- Frank Verheest (Gent, Belgium), Manfred Hellberg (Durban, S Africa), ...
- Miguel Bustamante & Fréderic Dias (Dublin, Ireland)
- John Dudley (Besançon, France), Norbert Hofmann (Imperial Coll., UK & Hamburg, Germany), ...

– ***Financial support***:

– FP7-PEOPLE-2013-IRSES (grant 612506 *QUANTUM PLASMAS*, 2014-2017);

– Brazilian Research Council (CNPq - Brasil) (*"Waves and Instabilities in Quantum Plasmas"*, 2013-2016);